University of Washington
Department of Civil and Environmental Engineering

ROUND HORIZONTAL THERMAL BUOYANT JET IN A CROSS FLOW

R. E. Nece
J. D. Littler

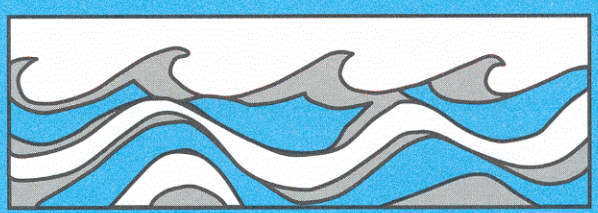

Water Resources Series
Technical Report No. 34
June 1973

Seattle, Washington
98195

Department of Civil Engineering
University of Washington
Seattle, Washington 98195

ROUND HORIZONTAL THERMAL BUOYANT JET IN A CROSS FLOW

R. E. Nece
E. P. Littler

Water Resources Series
Technical Report No. 34

June 1973

Addenda and Errata

ROUND HORIZONTAL THERMAL-BUOYANT JET IN A CROSS FLOW

by R.E. Nece and J.D. Littler

KEY WORDS: *Thermal pollution, *Jet diffusion, Hydrodynamics.

ABSTRACT: Results are presented for an experimental study of round buoyant jets discharged horizontally into and at right angles to the direction of flow of an unstratified receiving stream. Objectives of the study were to obtain empirical relationships defining the trajectory and near field temperature distribution of such jets.

Experimental results are given in the form of dimensionless jet trajectories and centerline temperature elevation above that of the receiving fluid. Experimental data were obtained for jet densimetric Froude numbers (as conventionally defined) of 5, 10, and 15, combined with jet discharge/cross flow velocity ratios of 0.5, 1, 5, and 10. The velocity ratio was found to be far more significant in determining the jet behavior than was the densimetric Froude number. Velocity ratios and Froude numbers tested span ranges commonly encountered in outfall designs.

Experimental parameters, including boundary conditions with the jet being discharged from a circular outfall located close to the bottom of the receiving channel, were intended to be representative of simplified approximations of a single-outfall cooling water discharge from a thermal plant located on a river. Effects of the near proximity of the channel bottom and of the small channel depth/jet diameter ratio of 4 were clearly evident in comparison of the results with those of previous cases of jets discharged into cross flows.

Errata

page 12, line 12: should read..."permanganate solution"

page 25, line 7 : should read..."negative y-coordinates"

page 28, line 17: should read..."negative y-coordinates"

page 52, third reference, should read:

Albertson, M.D., Y.B. Dai, R.A. Jensen and H. Rouse, 1950, "Diffusion of Submerged Jets," Transactions ASCE, 115, 639-664.

Charles W. Harris Hydraulics Laboratory

Department of Civil Engineering

University of Washington
Seattle, Washington 98195

ROUND HORIZONTAL THERMAL-BUOYANT JET IN A CROSS FLOW

By

Ronald E. Nece and John D. Littler

June 1973

Technical Report No. 34

Project Completion Report
OWRR Project Number: A-056-WASH
OWRR Agreement Number: 14-34-10E-3996-3027
Allotment Period: July 1, 1972-June 30, 1973

TABLE OF CONTENTS

ACKNOWLEDGEMENT

The work upon which this report is based was supported by funds provided by the United States Department of the Interior, Office of Water Resources Research as authorized under the Water Resources Research Act of 1964 through the State of Washington Water Research Center.

The study was conducted at the Charles W. Harris Hydraulics Laboratory, University of Washington. The experiments were performed by John D. Littler, Research Assistant, and served as the basis for Mr. Littler's MSCE thesis entitled "Thermal Diffusion of a Round Buoyant Jet Discharged into a Cross Flow". The work was directed by Ronald E. Nece, Professor of Civil Engineering (Principal Investigator).

ABSTRACT

Results are presented for an experimental study of round buoyant jets discharged horizontally into and at right angles to the direction of flow of an unstratified receiving stream. Objectives of the study were to obtain empirical relationships defining the trajectory and near field temperature distribution of such jets.

Experimental results are given in the form of dimensionless jet trajectories and centerline temperature elevation above that of the receiving fluid. Experimental data were obtained for jet densimetric Froude numbers (as conventionally defined) of 5, 10, and 15, combined with jet discharge: cross flow velocity ratios of 0.5, 1, 5, and 10. The velocity ratio was found to be far more significant in determining the jet behavior than was the densimetric Froude number. Velocity ratios and Froude numbers tested span ranges commonly encountered in outfall designs.

Experimental parameters, including boundary conditions with the jet being discharged from a circular outfall located close to the bottom of the receiving channel, were intended to be representative of simplified approximations of a single-outfall cooling water discharge from a thermal plant located on a river. Effects of the near proximity of the channel bottom and of the small channel depth: jet diameter ratio of 4 were clearly evident in comparison of the results with those of previous cases of jets discharged into cross flows.

LIST OF FIGURES

LIST OF FIGURES (Cont.)

LIST OF FIGURES (Cont.)

I. INTRODUCTION

Problems associated with the discharge of industrial, thermal, and sewage effluents into natural bodies of water such as streams and lakes have spurred much activity in the study of the fluid mechanics of turbulent jets. The objective of this report is to contribute information on one particular type of jet problem which might be encountered fairly commonly in engineering practice.

The particular problem investigated in this study is that of a round, horizontal, thermal-buoyant jet discharged at right angles into an unstratified cross flow. The variables of the problem are shown in Fig. 1.

The experimental study concentrated on determining jet centerline trajectories and jet centerline temperatures in the relatively close proximity of the outfall. The ranges of variables covered in the laboratory study are pertinent to design problems of thermal plants using once-through cooling and discharging warm condenser cooling water to streams through single outfalls placed near the stream bottom. The finite depth of the receiving stream, the relatively large jet discharge diameter compared to stream depth, and the effect of a finite discharge conduit placed within the partially confined channel flow together prevent the results of the study from being general in a fluid mechanics sense. However, the results do show which parameters are most influential on buoyant jet performance in a cross flow.

Data are presented in dimensionless form suitable for design calculations. The jet trajectory results are expressed in terms of the dimensionless centerline temperature elevation above the receiving stream temperature, $(T_{\ell} - T_a)/(T_o - T_a)$, and the dimensionless coordinates x/D, y/D (and to a lesser extent z/D) as influenced by the jet discharge: stream flow velocity

ratio B and the densimetric Froude number. These two independent parameters are defined as :

$$B = \frac{U_o}{V} \tag{1}$$

$$\mathbb{F} = \frac{V_o}{\sqrt{g \frac{\Delta\rho}{\rho_o} D}} \tag{2}$$

where $\Delta\rho = \rho_a - \rho_o$, the density differential between the ambient receiving stream fluid and the jet fluid at discharge. On the basis of relevant work reported in the recent literature, the experiments were performed at nominal B values of 0.5, 1, 5, and 10, and at nominal $\mathbb{F}$ values of 5, 10, and 15. Data were obtained for L/D values of 0 and 10. All results were obtained with $d/D = 4.0$ and $z_o/D = 0.67$.

The empirical results are presented in graphical form suitable for design calculations and from which comparison with other data in the literature might be made. No theoretical analysis was attempted.

The experimental results are confined to the near field, defined here as the region within the expanding and diffusing hot-water jet between the discharge nozzle exit (x, y, z, s = 0) and the location on the jet centerline where the jet becomes essentially parallel to the receiving stream velocity V.

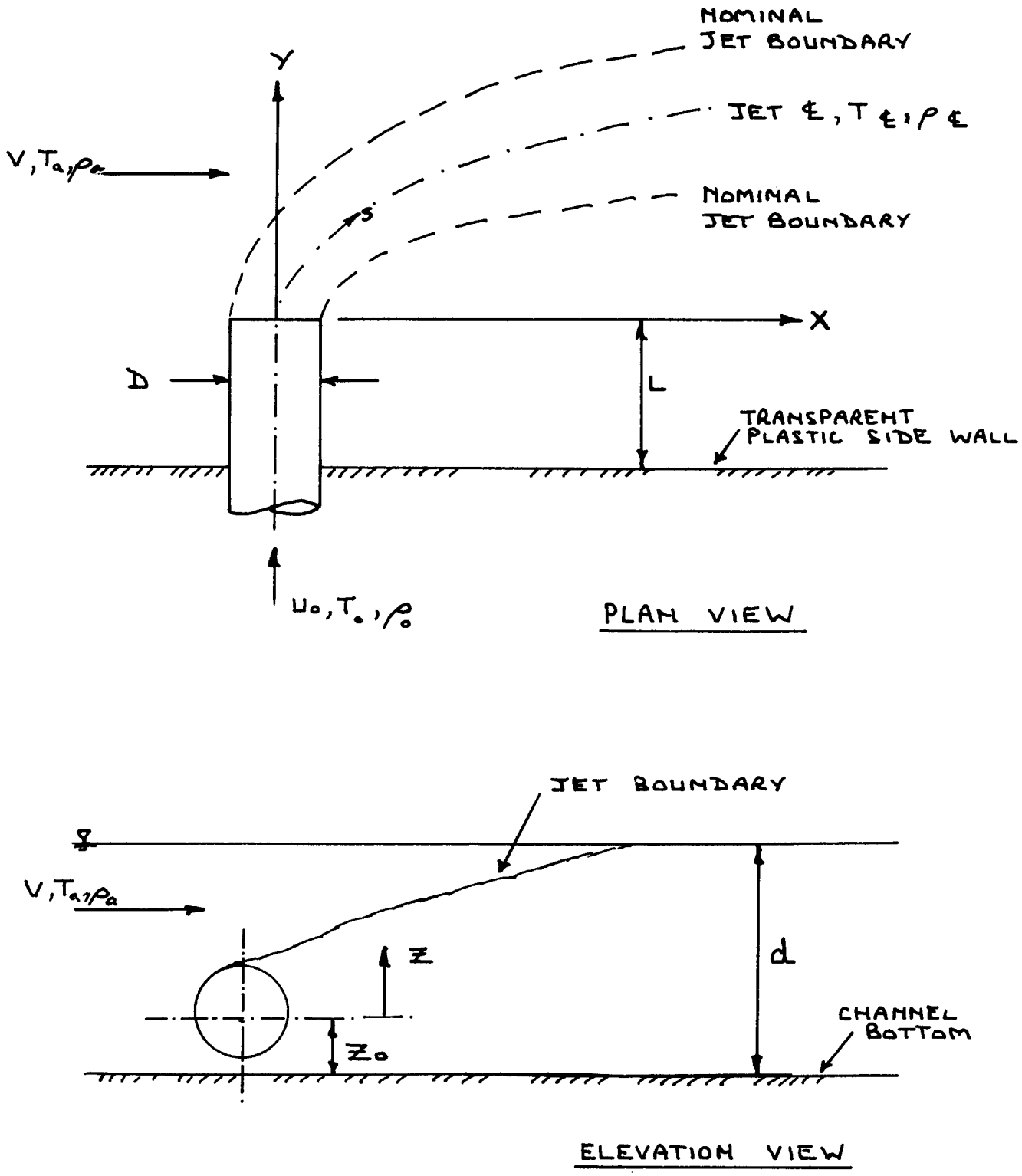

Figure 1. Definition and Notation Sketch

II. LITERATURE REVIEW

The following brief literature review is provided for the purpose of giving some background against which the present work may be positioned. There has been no attempt here to make a thorough review as the body of literature on turbulent jets is growing constantly as both basic studies of different jet-receiving fluid combinations and model studies applied to specific engineering projects are being reported continually.

In order to facilitate comparisons between various studies to be cited, turbulent jet problems will be classified as indicated in the list below. The review is restricted to consideration of round jets in unstratified receiving fluids, which was the case in the present study; even so, the list is incomplete as not all jet-cross flow direction combinations are listed.

Class 1: Non-buoyant jet into quiescent receiving fluid.

Class 2: Buoyant jet into quiescent receiving fluid.

Class 3: Non-buoyant jet into a cross flow.

Class 4: Buoyant jets into a flowing stream.

(a) Jet parallel to stream velocity, buoyancy force normal to jet discharge axis.

(b) Jet normal to stream velocity, buoyancy force parallel to jet discharge axis.

(c) Jet discharge axis, stream velocity, and buoyancy force mutually orthogonal.

The common analytical approach in the engineering literature has been to adopt an integral, control volume procedure in which Gaussian profiles of velocity and concentration (temperature excess, density deficit, or suspended material concentration) are assumed across the jet in the so-called

region of established flow where the original 'top-hat' velocity or concentration profile at the jet discharge point has completely eroded and centerline velocities or concentrations are lower than those at the nozzle discharge. Laboratory experiments have provided numerical values for the empirical constants incorporated in the analyses.

Class 1. This is the classical momentum jet. American engineering practice draws most heavily on the work of Albertson et al. (1950), from whose results the following equations for time-averaged velocity profiles in the region of established flow of the non-deflecting jet are obtained. Note that in these equations the notation has been made compatible with Fig. 1 in that the s-direction remains constant and is aligned with the initial direction of jet discharge.

$$\frac{u_m}{U_o} = 6.2 \frac{D}{S} \tag{3}$$

$$\frac{u}{u_m} = e^{-k(\frac{r}{s})^2} \tag{4}$$

where: u_m = centerline (maximum) velocity at axial station s

u = axial velocity at radius r from the jet centerline

The experimental value of k, using the results of Albertson et al. (1950) is 77.

Heat and material diffuse at different rates than does momentum. This is taken into account by writing the equivalent concentration distribution in the form

$$\frac{c}{c_m} = e^{-\mu k(\frac{r}{s})^2} \tag{5}$$

where: c_m, c = concentrations on the centerline and at radius r, respectively

μ = a 'sidesway coefficient'

For momentum jets a commonly used value of μ is 0.80, as cited by Abraham (1960). This leads in turn to the following equation for decay of concentration on the jet centerline, in the region of fully established flow.

$$\frac{c_m}{c_o} = 5.6 \frac{D}{S} \tag{6}$$

Strictly speaking, the momentum jet analysis applies only to the case $\mathbb{F} = \infty$, as defined by Eq. (2).

Class 2. Perhaps the most commonly accepted treatment of the buoyant jet in a quiescent receiving fluid follows the procedures outlined by Fan and Brooks (1966, 1969). Comparable results making use of a different computation procedure have been obtained by Anwar (1969). The numerical solutions presented make use of empirical values obtained by Rouse et al. (1952). Commonly employed values of μ and k are 0.74 and 96, respectively. For direct application to sewer outfalls, for example, results are typically presented in graphical form giving jet trajectories in the vertical plane and centerline dilution ratios, where the dilution ratio is defined as c_o/c_m, with $\mathbb{F}$ being the independent variable.

Class 3. Pratte and Baines (1967) delineated three zones for a non-buoyant jet entering at right angles into a cross flow: a potential zone, prior to the erosion of the centerline velocity below its initial discharge value, and thus comparable to the zone of establishing flow for $s/D < 6.2$ as given by Albertson et al. (1950) for the pure momentum jet; a zone of maximum deflection, in which the cross and jet flows mix rapidly, the jet centerline velocity decreases rapidly, and the wake eddies which appear on the downstream side of the jet in the potential zone expand and intensify

to occupy a large portion of the jet cross section as a pair of vortices; and a vortex region in which the vortices are carried along at the cross flow velocity. Chan and Kennedy (1972) have given further data on trajectories of non-buoyant jets in cross flows, as well as providing velocity distribution in the plane of symmetry of such jets in the zone of maximum deflection (or 'curvilinear' zone). The round, turbulent non-buoyant jet in a cross flow takes on a characteristic kidney-shaped cross section, as indicated in the sketch shown here.

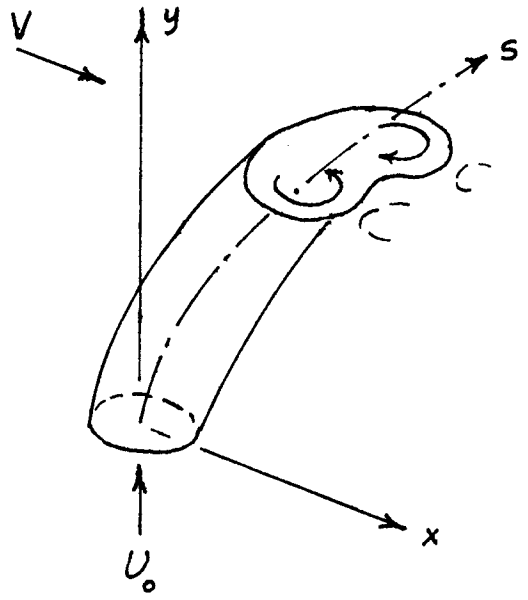

Class 4(a). Data for circular buoyant jets directed into co-flowing streams are limited; more data are available for the non-buoyant situation. Lomax (1971) presented limited temperature distribution data for a round, thermal-buoyant jet introduced by a nozzle aligned with the flow and located close to the bottom and on the centerline of a wide channel of finite depth. The d/D and z_o/D ratios were both very nearly the same as those used in the present study. Photographic data show that for a constant value of $B = U_o/V$, an increase in $\mathbb{F}$ produced in the test rig by an increase in jet temperature increased the lateral spread of the diffusing jet near the surface of the channel, and that for a constant $\mathbb{F}$ an increase in B likewise increased the lateral spread.

Class 4(b). A considerable body of literature exists on round buoyant

jets directed normal to the stream velocity and in which the direction of the buoyancy force is parallel to the jet discharge axis - i.e., the buoyancy force lies in the x-y plane defined in Fig. 1. A summary of jet trajectory equations obtained for classes 3 and 4(b) has been given by Chan and Kennedy (1972); empirical trajectory expressions, some from sources cited by Abramovich (1963), generally incorporate the velocity ratio B as a variable. Hirst (1972) has summarized some centerline velocity and concentration results for some class 3(b) experiments. Fan (1967) has presented a comparison of theoretical and experimental results for jet trajectories, widths, and dilution ratios, with the relevant parameters being F and B.

Class 4(c). No data were found in the general literature for this case. Some limited results had been given by Nece and Kent (1971) for the class 4(c) jet, where test data were reported for the case of $F = 10$, $B = 2.45$. The experiments were run in the same channel used in the present study, with L/D ratios of 7.6 and 0, d/D ratios of 2 and 4, and with the same $z_o/D = 0.67$. This 1971 investigation, which was a model study dealing with the simulation of the movement of juvenile downstream migrant salmon past a cooling-water discharge jet, provided the specific movitation for the present study.

This brief review indicates that the results given here apply to a case which the investigators did not find reported upon in the literature, and also provides a rationale for conducting the tests under systematically varied values of both F and B.

III. EXPERIMENTAL APPARATUS AND METHODS

Apparatus

The test facility was provided with two separate flow systems, for the receiving water and for the discharge jet.

The receiving water was supplied from the laboratory main circulation system. Water was delivered to the model from a constant head tank through a 6-inch pipe containing a flow meter (Dall tube) which measured flows in the 'cross flow' channel. The supply pipe discharged into a baffled head box attached to the flow channel through a faired transition. The test channel was 12 feet long, 4 feet wide, with a horizontal wood bottom painted white for visibility purposes and transparent plastic sidewalls 10 inches high. Flow rates were controlled by a valve on the supply pipe to the head box; channel water depths were controlled with an adjustable weir at the downstream end of the channel. The channel is shown in Fig. 2.

The warm water comprising the jet flow was supplied from a separate recirculatory system incorporating a pump, a constant head tank, and a partially insulated warm-water reservoir. Warm water was obtained from a hose connection to the laboratory domestic hot water supply. A 3-kilowatt partially immersible heater, mounted on a floating base, was used to maintain temperatures of the jet supply water in the 17-cubic foot capacity reservoir. Reservoir temperatures were monitored by a sealed immersible thermometer with a dial gage. Jet discharges were regulated by valves between the constant head tank and the outfall conduit; flow rates were measured with a 5/8-inch throat venturi meter in the conduit supply line.

The jet outfall conduit was formed by a 1.5-inch I.D. plastic tube inserted through a sleeve in one channel side wall at a station 3 feet downstream

from the channel entrance. The tube was longitudianlly adjustable in the sleeve in order to make varous jet discharge axial positions L possible. The sleeve acted as a spacer between the plexiglass tube and the channel bottom, so that the axis of the 1.75-inch O.D. tube was at a vertical spacing of 1 inch above the bottom; the z_o/D ratio thus was fixed at 0.67.

Temperature readings were the only data taken in the jet. The temperature probes were mounted on an instrument carriage assembly riding on horizontal, parallel steel rails attached to the tops of the channel walls. The six temperature sensors were YSI No. 401 thermistor probes having a 7-second time constant. Each probe could be adjusted to a desired y-coordinate. During testing the probes were aligned at the same level so that the z-coordinates of all probes were set equal and then were changed equally as the cross member supporting the probes was raised or lowered by means of a rack and pinion arrangement attached to the instrument carriage. The carriage could be clamped in place at any desired x-station for the probe array. The instrument carriage and probe array are shown in Fig. 3.

The temperature sensors were connected to a YSI switch box, which in turn was connected to a single YSI Model 43 Thermistemp Tele-Thermometer. The tele-thermometer had a temperature range of 0°-50° C, with an accuracy of 1% of the scale range (0.5°C) and a readability of 0.2°C for direct visual readout of temperatures.

Test Ranges and Procedures

All tests were run at a regulated channel depth d = 6 inches; therefore, d/D = 4.0 for all runs.

The methodology outlined below was followed for each [illegible] - B combination. Channel and jet discharges were set to obtain the specified V and U_o values;

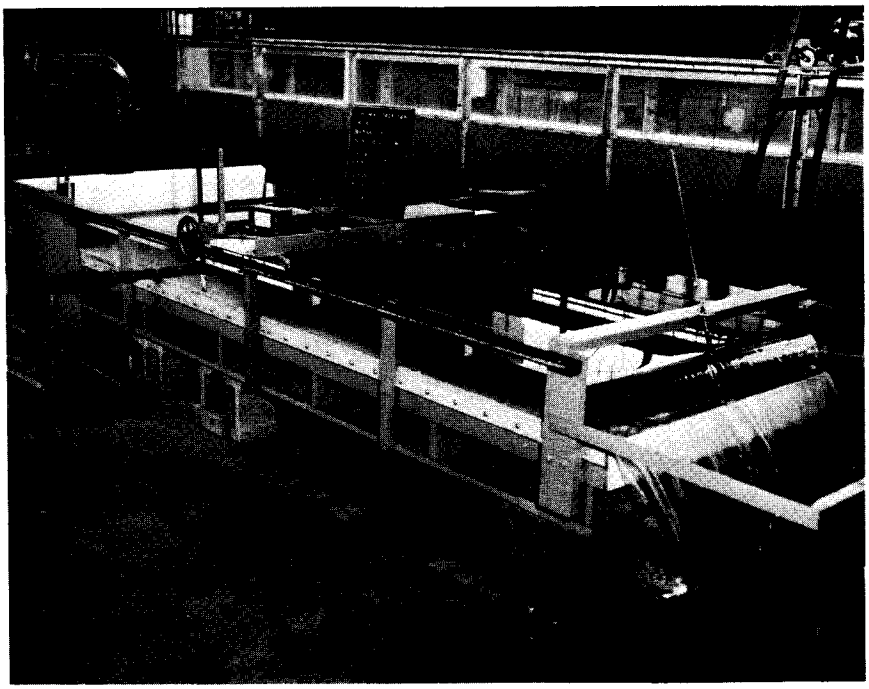

Figure 2. Side View Photograph of Channel and Carriage

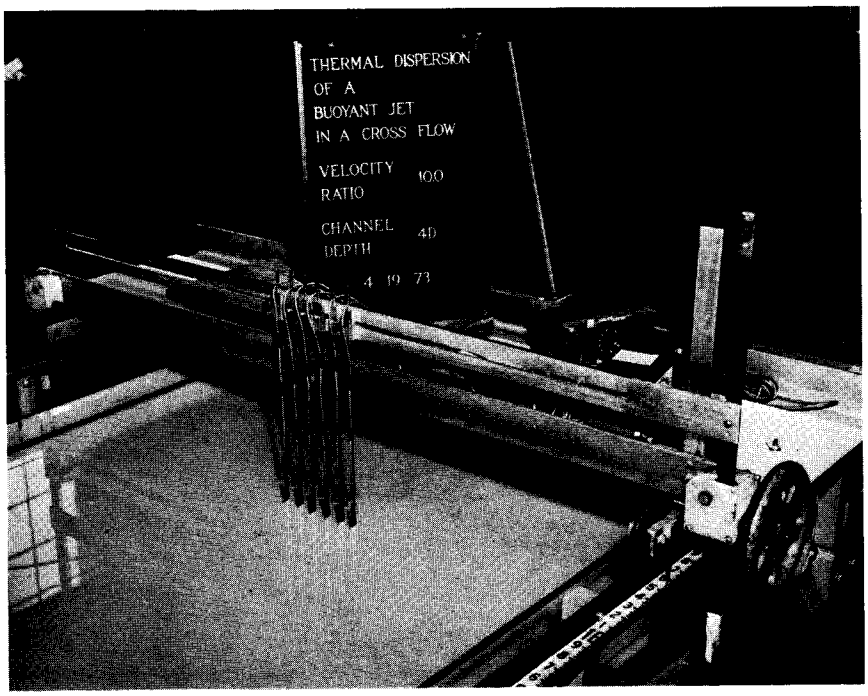

Figure 3. Upstreamm Closeup Photograph of Instrument Carriage and Probes

these values were taken as spatial averages, applying the one-dimensional continuity equation to the metered discharge rates through channel and conduit sections. Setting the specified F required adjustment of the jet water temperature with respect to the temperature of the channel flow; standard tables relating water temperature to density were employed. Temperature differentials between jet and channel discharges were maintained at values comparable to those experienced in thermal plant cooling-water discharges. Channel flow and jet temperatures, the latter taken just inside the outfall conduit, were measured with a seventh, hand-held, thermistor. The warm water in the jet supply was dyed with potassium permanagante solution to allow visual observations.

Temperature field data were taken at six downstream stations, at x/D stations of 1/2, 1, 2, 4, 8, and 16. At each x-station, the six rack-mounted thermistors were placed, by visual inspection, at locations across the channel best spanning the jet centerline at that x-station. The probes were then spaced approximately symmetrically about the jet centerline, so that they were spaced at equal distances between the jet centerline and the jet boundary as approximated by the dye outlines.

The emphasis in the test program was on location of the jet centerline, taken as the point in the jet cross section where the temperature was maximum, and on the value of the centerline temperature. Accordingly, only sufficient temperature readings were taken to determine these two items. The customary procedure was to record 24 point temperature values, 6 at each of 4 depths above the channel floor, and by interpolation determine the location and the value of the maximum temperature in the plane of the x-station. Complete temperature contours thus were not determined over the entire jet or over the entire depth. These temperature data are not detailed in this report,

but are on file. Jet and channel flow temperatures were taken before and after temperature contours were measured at each x-station so that variations in the temperature sensitive Froude number could be determined.

When all temperature readings were completed for a given $\mathbb{F}$ - B combination, sketches of the jet plan and side elevation views were made from visual observations of the dyed jet.

Most data were taken at L/D = 10, with the finite length of conduit in the channel flow. At this L/D, tests were made at $\mathbb{F}$ = 5, 10, and 15 for B values of 0.5, 1, and 5, and for $\mathbb{F}$ = 10 and 15 for B = 10. Due to limits on velocities which could be obtained in the channel and in the jet, it was not possible to make a run with a B = 10 in combination with $\mathbb{F}$ = 5. One intermediate run was made at B = 2.5, $\mathbb{F}$ = 10. Tests at L/D = 0, for which the conduit nozzle was flush with the channel sidewall, were limited to runs at $\mathbb{F}$ = 5, 10, and 15 for B = 0.5, and for B values of 1, 5, and 10 for a constant $\mathbb{F}$ = 10.

Figures 4 and 5 show photographs of the dyed jet for the L/D = 10 case for B values of 0.5 and 10, respectively.

Data Reduction

All data were reduced to dimensionless form. Jet trajectories in the horizontal plane were expressed graphically in terms of x/D vs. y/D, plotted for the various $\mathbb{F}$-B combinations. It is emphasized that all of the jet characteristics are based on temperature measurements alone, and specifically upon interpolation within each x-station temperature contour determination to determine the location of the jet centerline as defined by the point of maximum temperature. Each individual point on a trajectory plot thus required the drawing of isotemp lines in the 24-point temperature plot in each

Figure 4. Plan View Photograph of Jet, L/D = 10 and B = 0.5

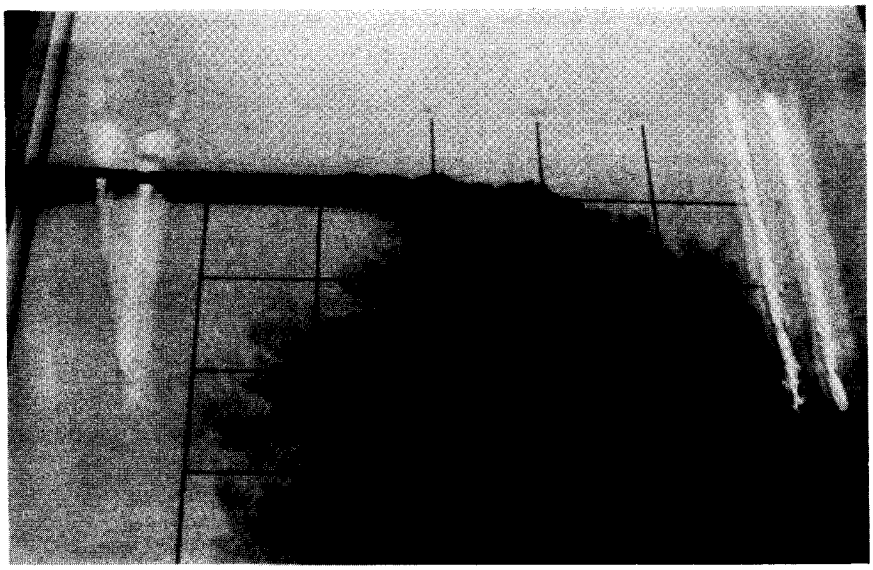

Figure 5. Plan View Photograph of Jet, L/D = 10 and B = 10.0

x-station plane.

Jet centerline temperatures were correlated in terms of a dimensionless temperature excess parameter, T, defined as follows:

$$T = \frac{T_{\ell} - T_a}{T_o - T_a} \tag{7}$$

where: T_{ℓ} = temperature on jet centerline

T_o = jet temperature at nozzle exit

T_a = temperature of the ambient channel cross flow water

The temperature parameter T was correlated with the dimensionless coordinate s/D, where s is measured along the curvilinear jet axis as shown in Fig. 1. This choice put the results in a form compatible with those reported for other jet configurations.

Reynolds numbers were determined for both the jet and channel flows, and were defined as follows:

$$\text{Jet Flow: } \mathbb{R}_i = \frac{U_o D}{\nu} \tag{8}$$

$$\text{Cross Flow: } \mathbb{R}_c = \frac{Vd}{\nu} \tag{9}$$

where ν is the kinematic viscosity of the fluid. During the tests the jet Reynolds number $\mathbb{R}_i$ ranged from approximately 6,000 to 12,500, well within the fully turbulent range. For the channel, $\mathbb{R}_c$ ranged approximately from 2,900 to 41,000, indicating that the channel flow was within the turbulent range throughout. Higher values of $\mathbb{R}_c$ for the constant depth runs correspond to the higher channel velocities. The turbulence induced in the channel flow by the head tank baffles was observed to be dependent upon the channel flow rate, but no turbulence measurements were made. Values of both $\mathbb{R}_i$ and $\mathbb{R}_c$ are considered sufficiently high so that test results are independent of

Reynolds number effects.

The primary data for the study are given in the Appendix. The values of $\mathbb{F}$ and B listed are nominal values; more precise values of B can be calculated from the tabulated U_o and V values. Values of $\mathbb{F}$ can be calculated from the given values U_o, T_a, and the T_o value at the time when temperature measurements were being taken in each specified plane of x = constant. The actual centerline temperatures as found from the temperature contour plots at each x-station are listed, as well as the dimensionless temperature parameter T and the corresponding centerline coordinate y/D at each x/D. The s/D coordinates were measured from x-y trajectory plots. The actual $\mathbb{F}$ values for each x/D data set for each $\mathbb{F}$-B combination are not listed, but ranges of actual values are listed on the data plots discussed in the next section.

IV. EXPERIMENTAL RESULTS

Jet Trajectory

Jet centerline trajectory data for L/D = 10 are shown on Figs. 6, 7, 8 and 9; these plots are for B values of 0.5, 1, 5, and 10, respectively. For each of the velocity ratio sets four curves are drawn, one for each of the nominal $\mathbb{F}$ values of 5, 10, and 15, and a dashed curve representing the average behavior for the set. Actual ranges of $\mathbb{F}$ applicable during the tests and associated with each nominal $\mathbb{F}$ value are indicated in parentheses on the diagrams. The exception to this correlation procedure is a missing value for the B = 10, $\mathbb{F}$ = 5 combination, which as already noted could not be obtained because the required channel flow could not be obtained because of supply limitations. From the curves of Figs. 6-9 it is apparent that the value of $\mathbb{F}$ has no significant effect on the jet centerline trajectory; the governing factor is clearly the velocity ratio B. Further comments about additional entries on Fig. 7 are given later.

In Fig. 10 the average jet centerlines for L/D = 10, as taken from Figs. 6-9, are plotted for purposes of comparison. Figures 11 and 12 show sketches of the jet plan and side elevation views for B values of 0.5 and 10, respectively. These are the same flow conditions shown in the photographs, Figs. 4 and 5, respectively, and represent conditions for the extremes of B tested. The grid marking on the channel bottom in the photographs employs 6-inch (4D) spacing. For B = 0.5, the jet behavior is strongly influenced by the boundary condition imposed by the presence of the relatively large outfall conduit which presents a large projected area to the channel flow. This is a consequence of the finite L/D and the relatively small d/D. The strong separation eddy, or vortex, which forms on the downstream side of the conduit at its

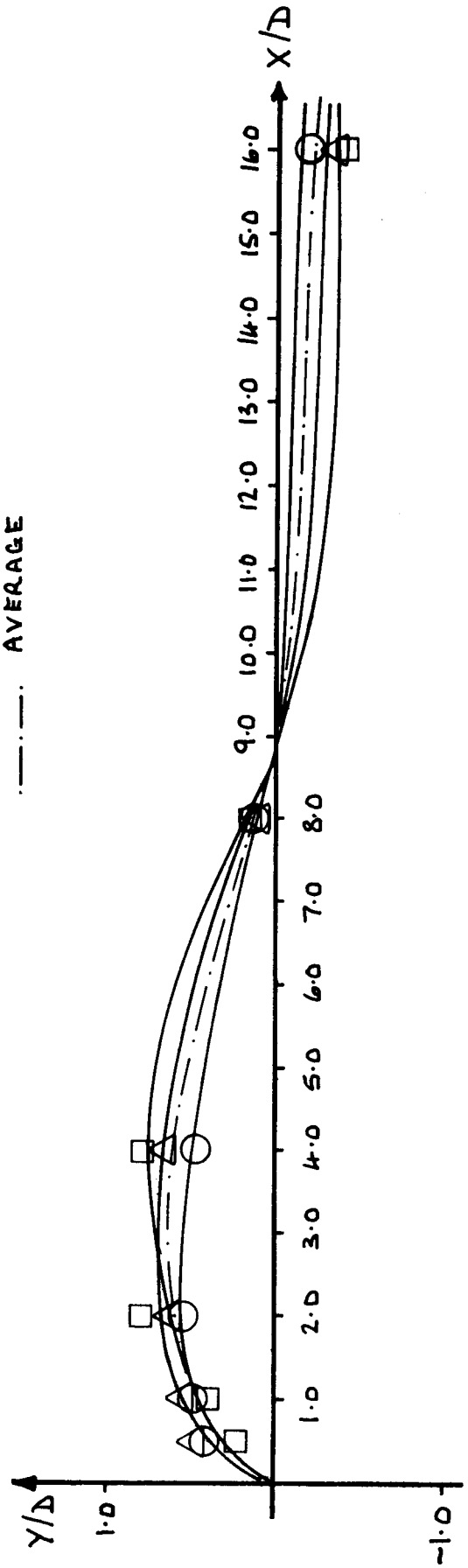

Figure 6. Plot of Jet Centerline Trajectories for B = 0.5, L/D = 10.0 and Variable FF.

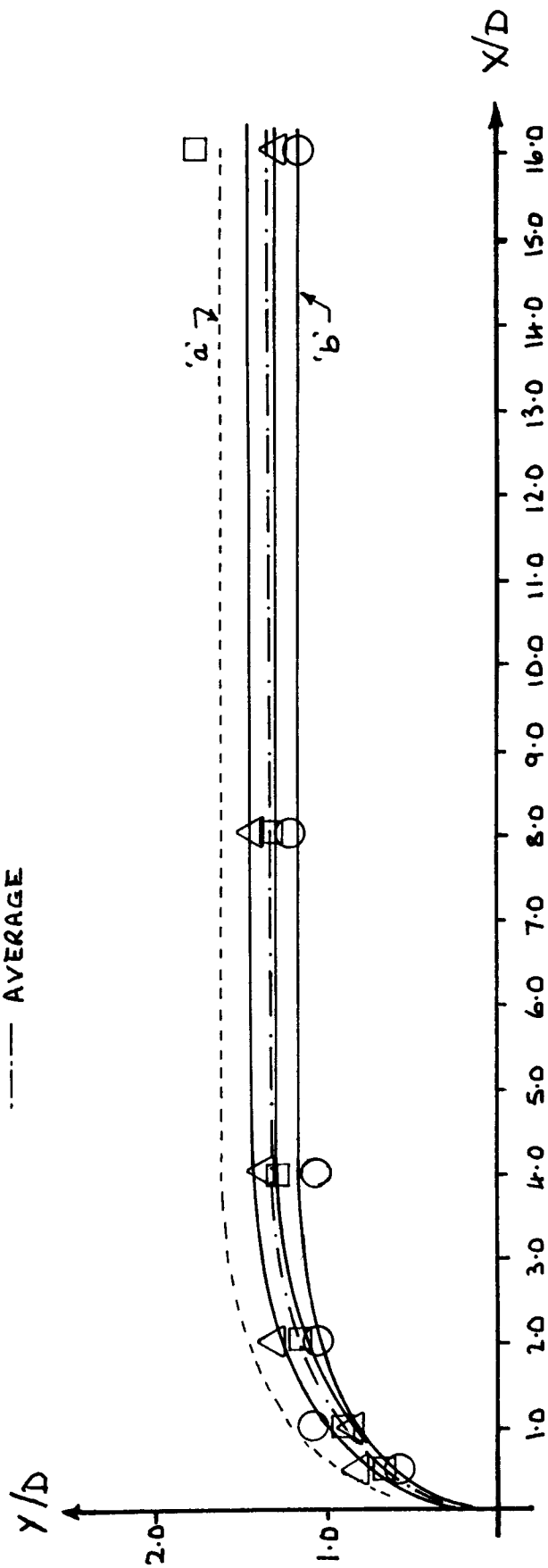

Figure 7. Plot of Jet Centerline Trajectories for B = 1.0, L/D = 10.0 and Variable FF.

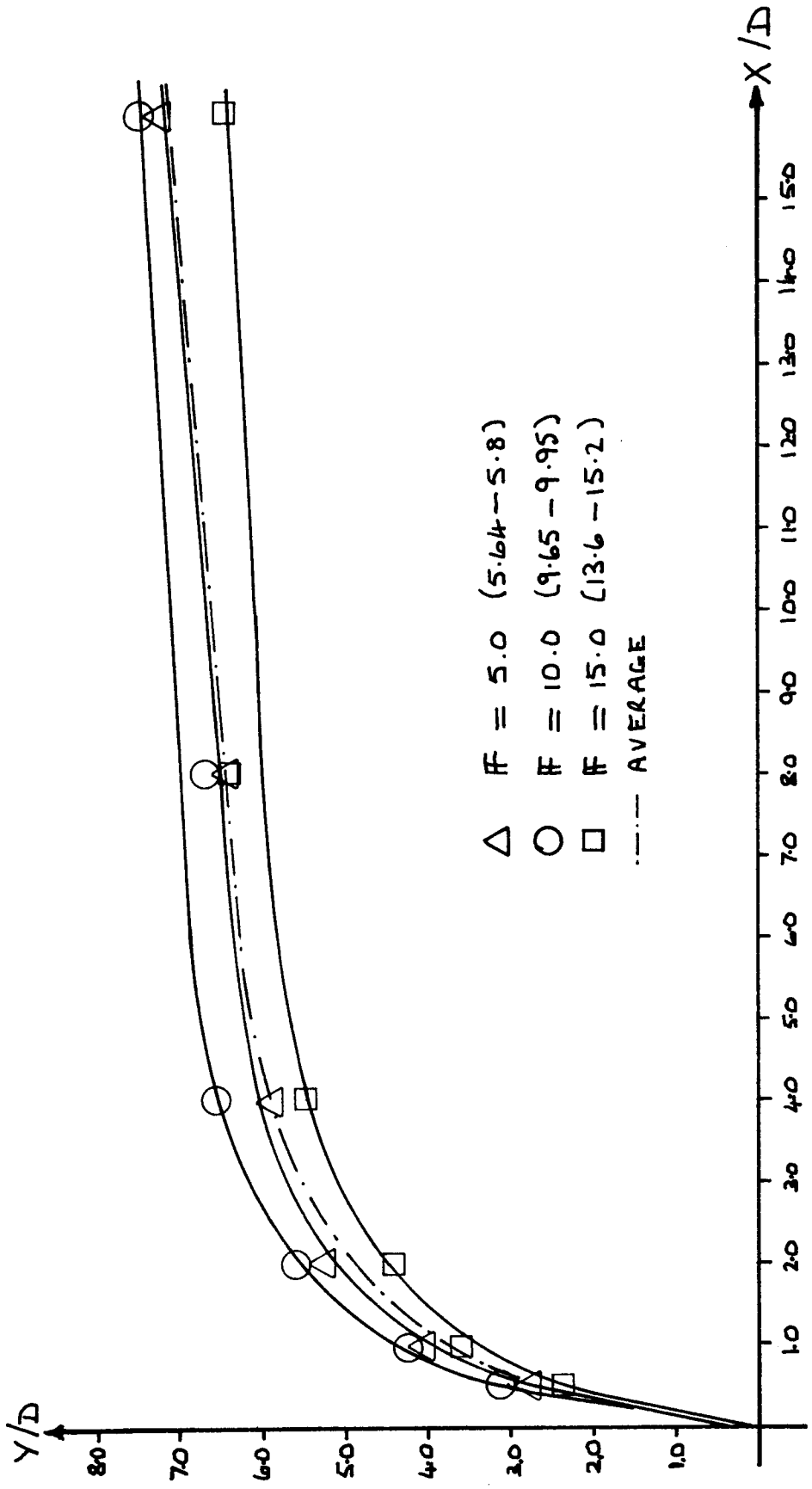

Figure 8. Plot of Jet Centerline Trajectories for B = 5.0, L/D = 10.0, and Variable ff .

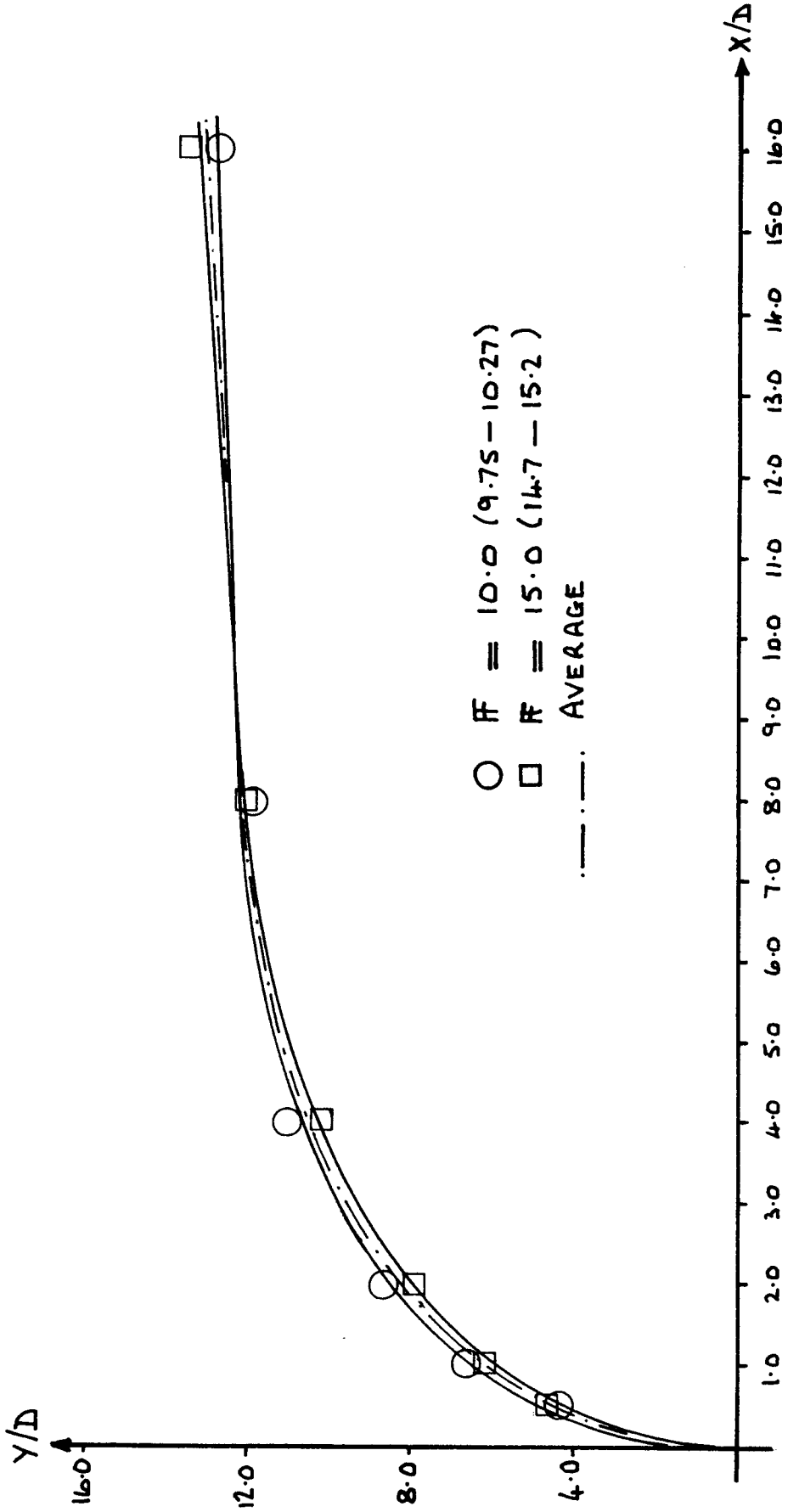

Figure 9. Plot of Jet Centerline Trajectories for B = 10.0, L/D = 10.0, and Variable FF.

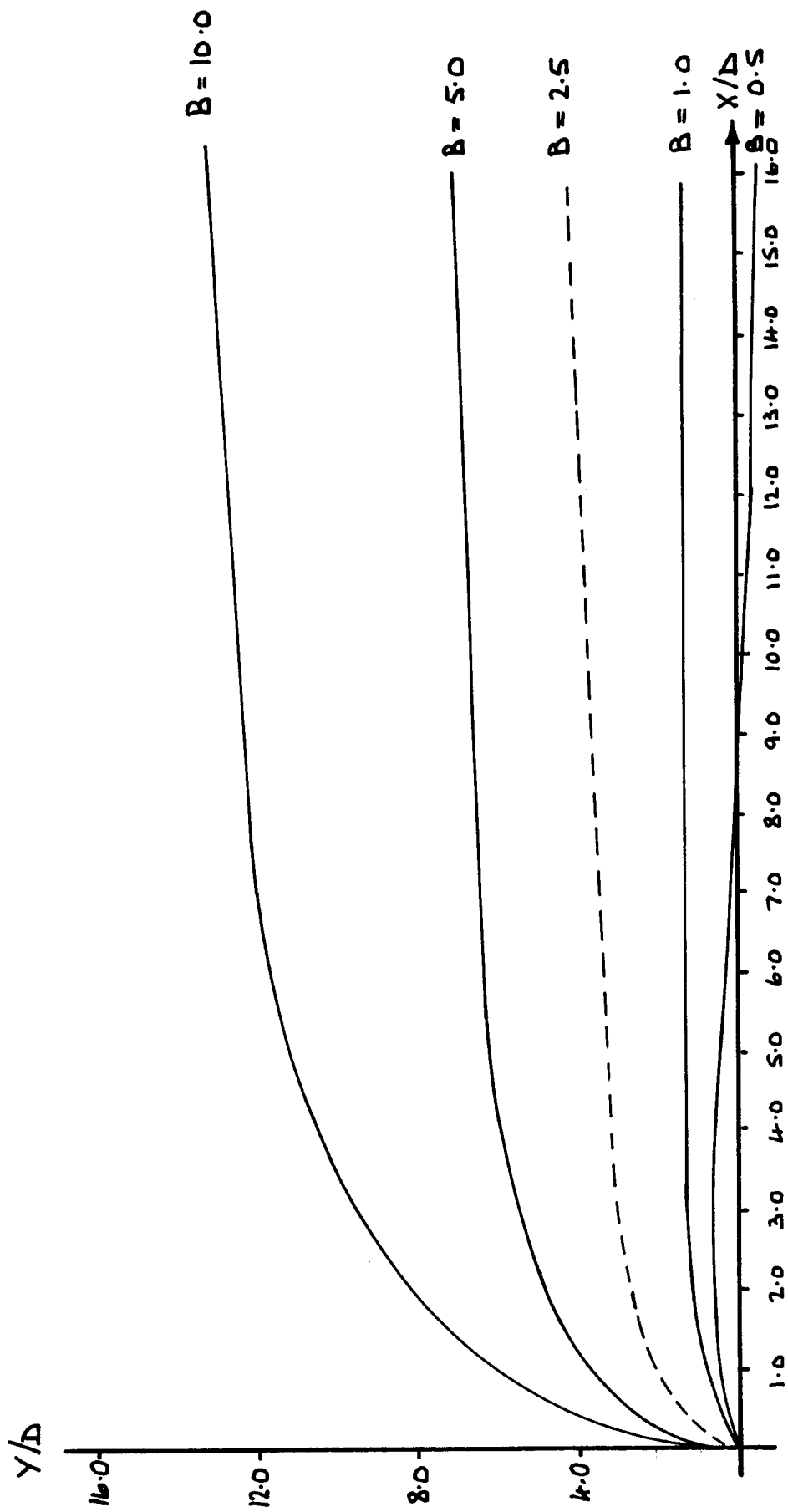

Figure 10. Plots of Average Jet Centerline Trajectories for the Various Velocity Ratios.

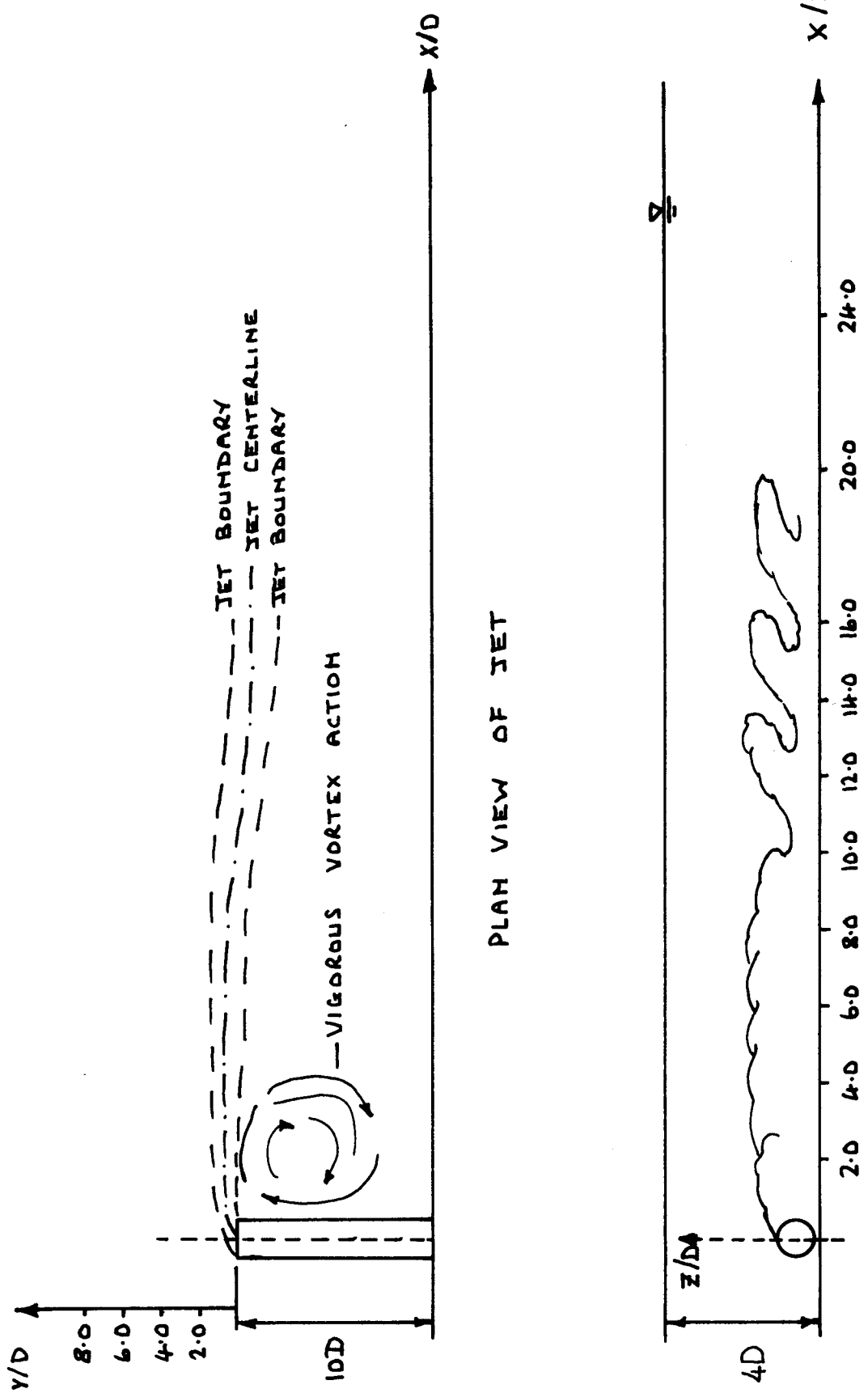

Figure 11. Jet Side Elevation and Plan View for B = 0.5, L/D = 10.0

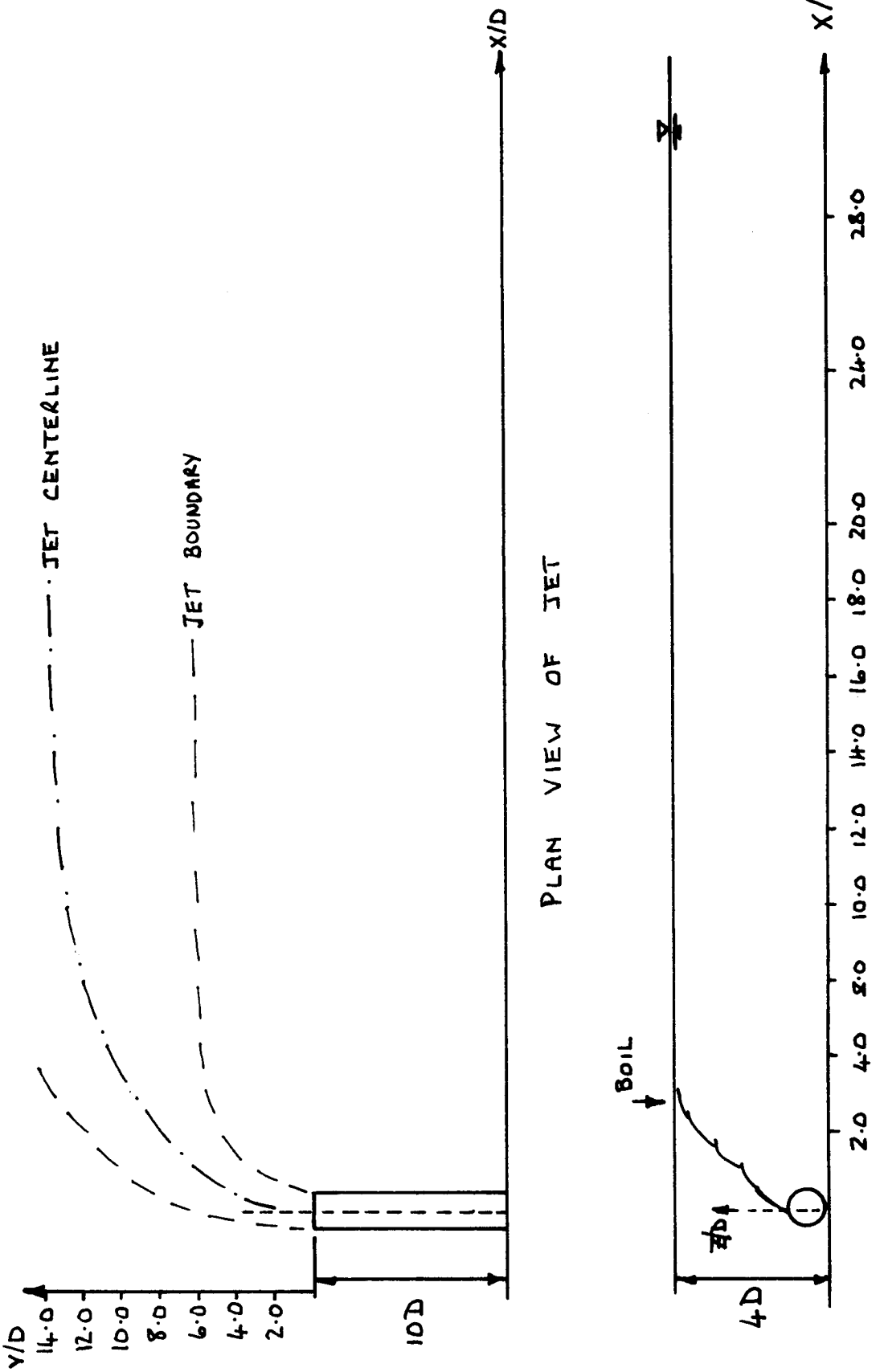

Figure 12. Jet Side Elevation and Plan View for B = 10.0, L/D = 10.0.

discharge end has a significant effect upon jet behavior at low jet discharge velocities - i.e., low B values. The relatively small U_o does not allow the jet to penetrate a significant distance into the cross flow, and the vortex at the downstream side of the outfall conduit induces a velocity in the edge of the jet and imparts angular momentum to it with the result that the jet is given a velocity component back toward the near channel wall. As a result, the jet centerline acquires some negative-y coordinates downstream from the discharge point. The separation eddy became less influential on jet performance as B increased.

For B = 0.5 the warm water jet did not rise a significant distance above the channel bottom. Two factors contribute to the essentially horizontal motion of the jet. The major influence is the (really three-dimensional, complex) separation eddy at the end of the conduit, coupled with the nature of the free stream flow, which itself is confined by the near proximity of the water surface. The combination produces a strong spiral current downstream from the conduit, and into which the jet flow is swept.

The second factor tending to keep the buoyant jet from rising was present in all of the runs. The jet was discharged in all cases with an initial vertical clearance of 0.17 D between the channel bottom and the lower edge of the round jet. Close to the nozzle the jet behaves much as a cylinder placed within the cross flow, and the pressure and cross flow fluid velocity distributions about the jet would be much like those around a comparable solid cylinder; analytical attacks on the problem such as those of Fan (1967) incorporate empirically obtained drag coefficients on such deflecting cylinders in momentum analyses. The small initial clearance between the jet and the channel floor leads to higher local cross flow velocities and in turn to lower pressures

under the jet than would be the case if the jet were discharged into an infinite fluid. Consequently, this additional boundary condition of the present study tended to decrease rise rates of the jets throughout the entire series of tests, imparting a tendency for the jets to remain close to the bottom.

By comparison, for B = 10 the jet rises much more rapidly and creates a 'boil' where the upstream edge of the jet visibly intersects the water surface at a relatively short distance (x/D = 3) downstream. The vertically asymmetric pressure distribution described above is still effective, however; the vertical rise z/D required for the jet centerline to intersect the water surface in the channel is smaller than is the case for equivalent axial distances x/D for buoyant jets in quiescent receiving fluids at comparable F values as indicated by trajectory data given by Anwar (1969).

There was no apparent effect of lateral confinement of channel sidewalls on the y-coordinates of the jets.

In order to check the reliability of the results shown in Figs. 6-9, the results for an intermediate combination of F = 10, B = 1 were selected for verification. The run was completed once by duplicating approximately the physical conditions - velocities and jet-channel flow temperature differential - and once by changing the physical conditions but maintaining the same nominal F-B combination. The trajectory comparison is shown on Fig. 13, where the smoothed curves only are shown; the actual numerical values obtained are shown on the first page of the appendix, identified at the bottom of the data columns by the letters 'a', 'b', and 'c'. Run 'a' was an early run, made when the experimental techniques were being developed, run 'b' was the near duplication of physical variables, and run 'c' was with different physical variables.

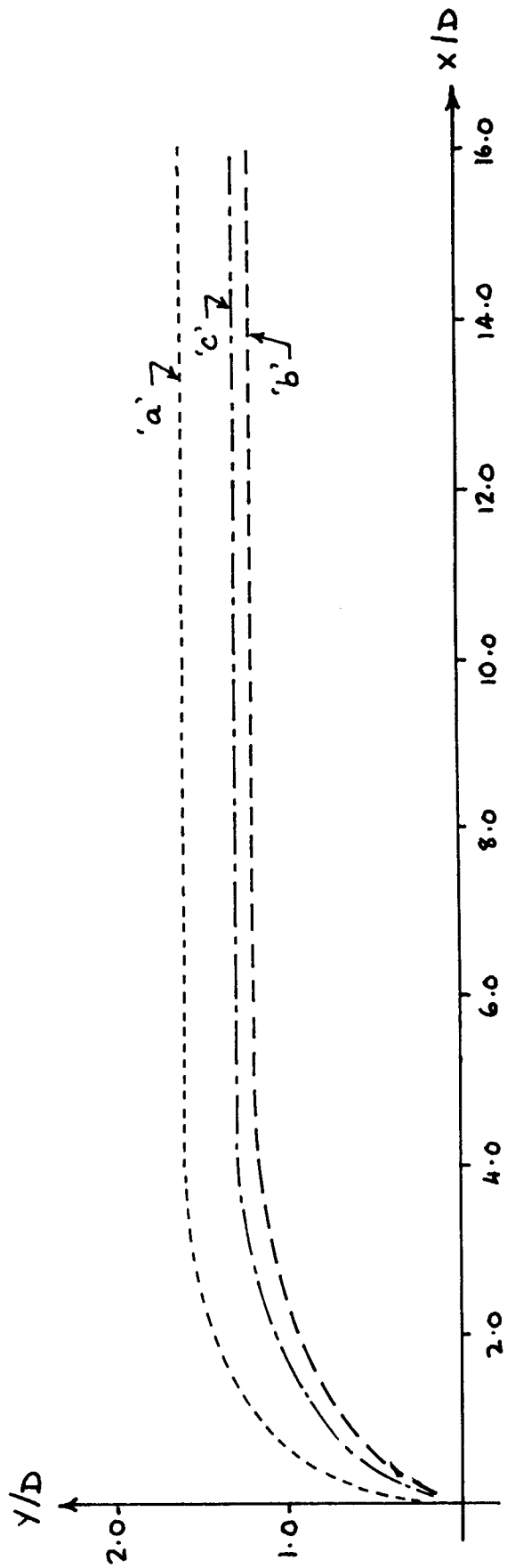

Figure 13. Plot of Jet Centerline Trajectories for Three Separate Runs Duplicating the Same Dimensionless Parameters, R = 1.0, $\mathbb{F}$ = 10.0, L/D = 10.0

The trajectory agreement between 'a' and the two later runs was not too good, although temperature comparisons (to be discussed later) were better. Runs 'b' and 'c', taken later in the test program, show good dimensionless correlation. The spread in the y/D values of about 0.5 at the downstream stations indicates a spread of about 3/4-inch in physical location of the jet centerline. The data for the three runs are all included in the 'average' curves for this $\mathbb{F}$-B combination shown on various plots. The data plotted on Fig. 7 are for run 'b'; run 'a' results are shown by the dotted line, and run 'c' is not shown because it is nearly coincident with the 'average' curve.

In order to examine the effects of the proximity of a sidewall to the jet discharge, a second series of tests but involving fewer total runs was made for an L/D ratio of zero, i.e., with the conduit discharge nozzle flush with the sidewall. Figures 14, 15, 16, and 17 show the resulting centerline trajectories along with the average centerline trajectories for corresponding velocity ratios B at L/D = 10.

In Fig. 14 centerline trajectories for $\mathbb{F}$ values of 5, 10, and 15 for B = 0.5, which was the case giving the negative-y coordinates of the jet centerline downstream for the L/D = 10 configuration. For the L/D = 0 case the nearby wall had a definite effect, lateral movement of the jet was restricted, and jet mixing was reduced. This restriction is shown in the plan and elevation view sketches of Fig. 18. There was, of course, no vortex associated with flow past a protruding conduit. The test data indicate that there was no noticeable effect of $\mathbb{F}$ on the jet trajectory. Accordingly, runs at the other B values were limited arbitrarily to a nominal $\mathbb{F}$ = 10 value. The data of Figs. 15-17 indicate close agreement between results for L/D = 10 and L/D = 0. As Fig. 15 applies for B = 1, a conclusion to be drawn is that

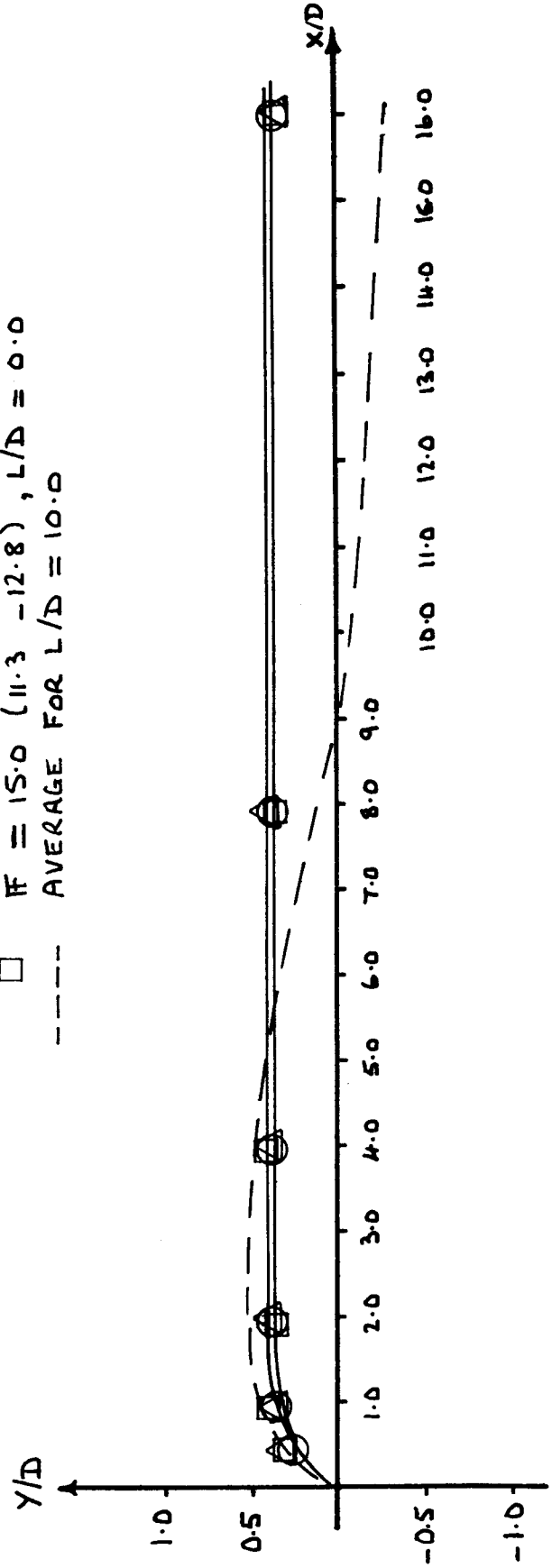

Figure 14. Comparison of Jet Centerline Trajectories for B = 0.5, L/D = 0.0 with the Average Jet Centerline Trajectory for B = 0.5, L/D = 10.0.

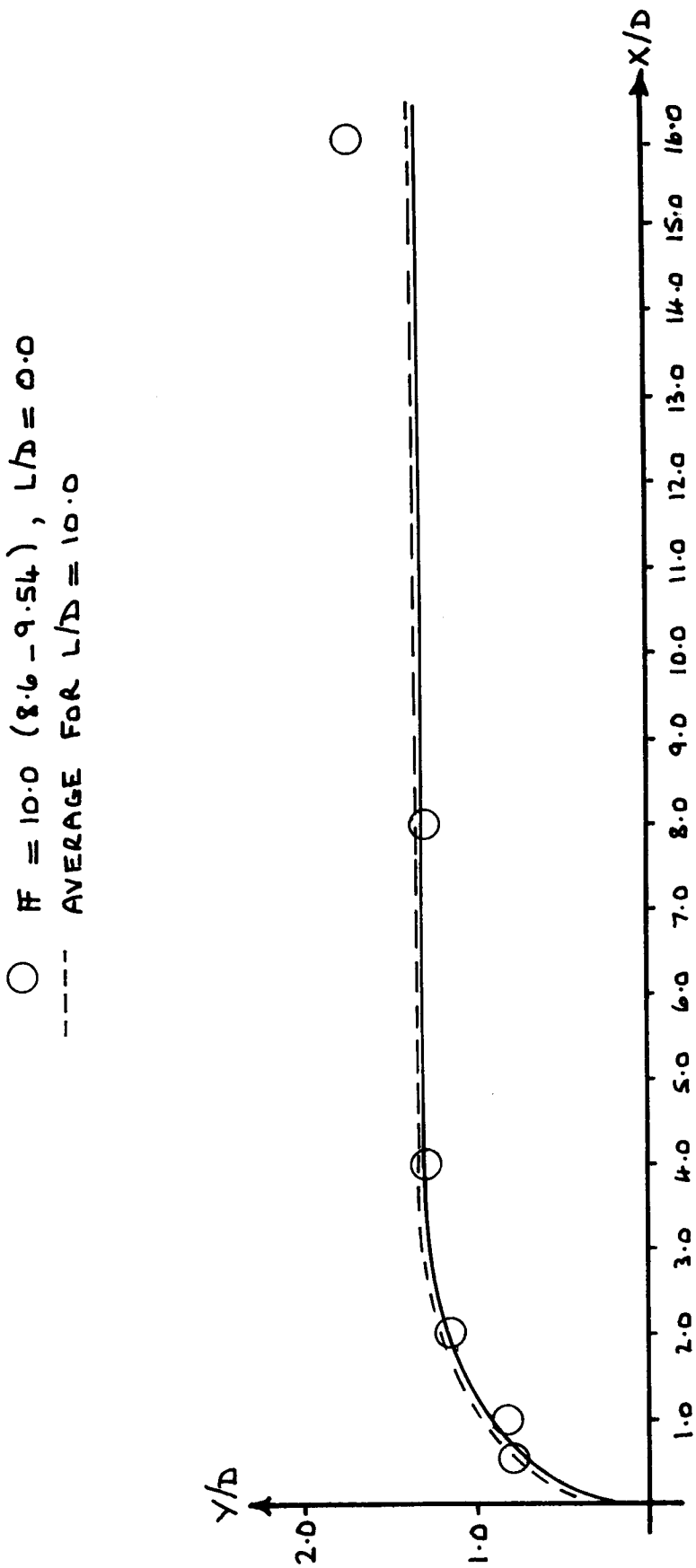

Figure 15. Comparison of Jet Centerline Trajectories for ff = 10.0, B = 1.0, L/D = 0.0 with Average for B = 1.0, L/D = 10.0.

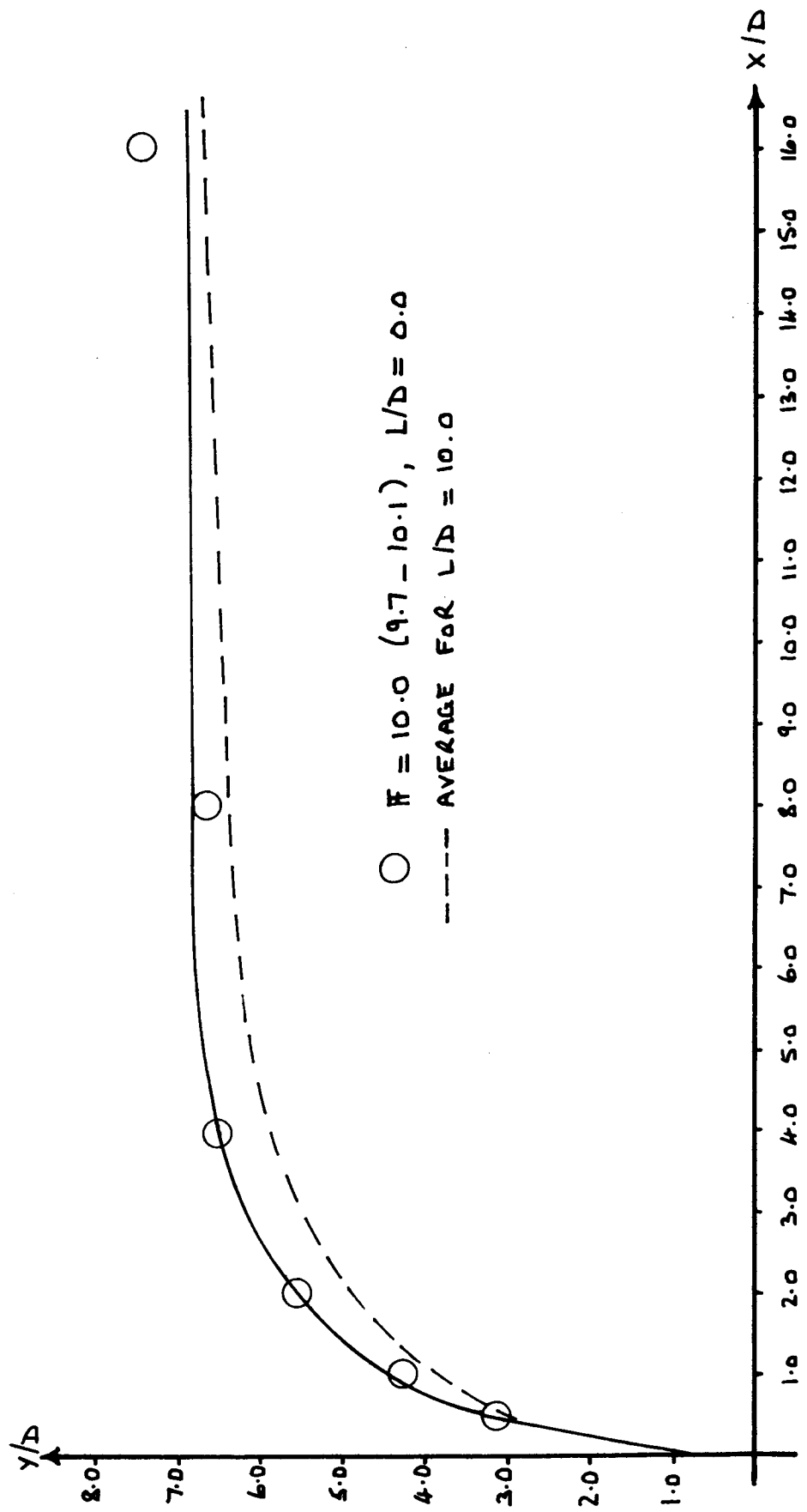

Figure 16. Comparison of Jet Centerline Trajectories for F = 10.0, B = 5.0, L/D = 0.0 with the Average for B = 5.0, L/D = 10.0.

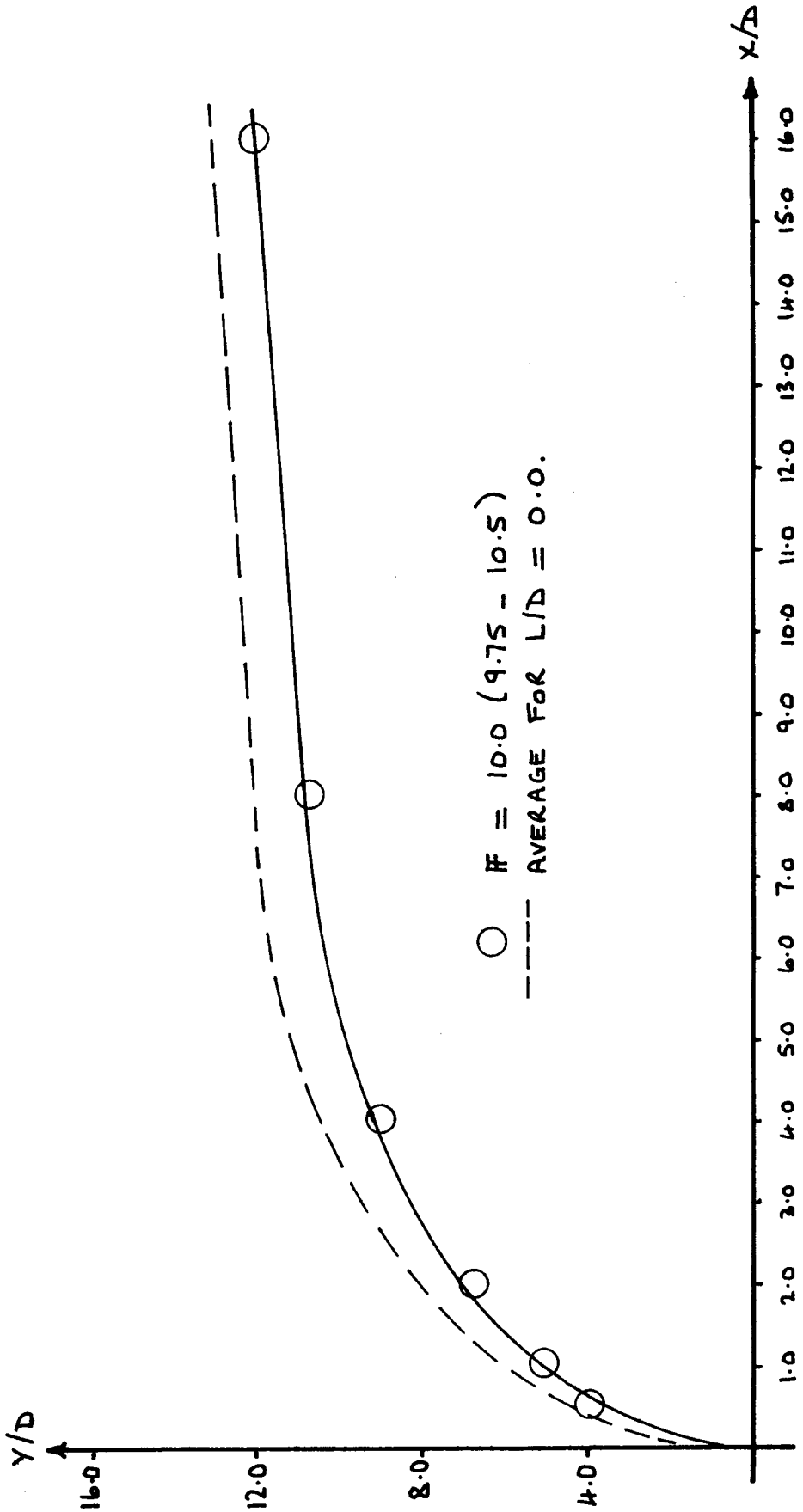

Figure 17. Comparison of Jet Centerline Trajectories for FF = 10.0, B = 10.0, L/D = 0.0 with the Average for B = 10.0, L/D = 10.0.

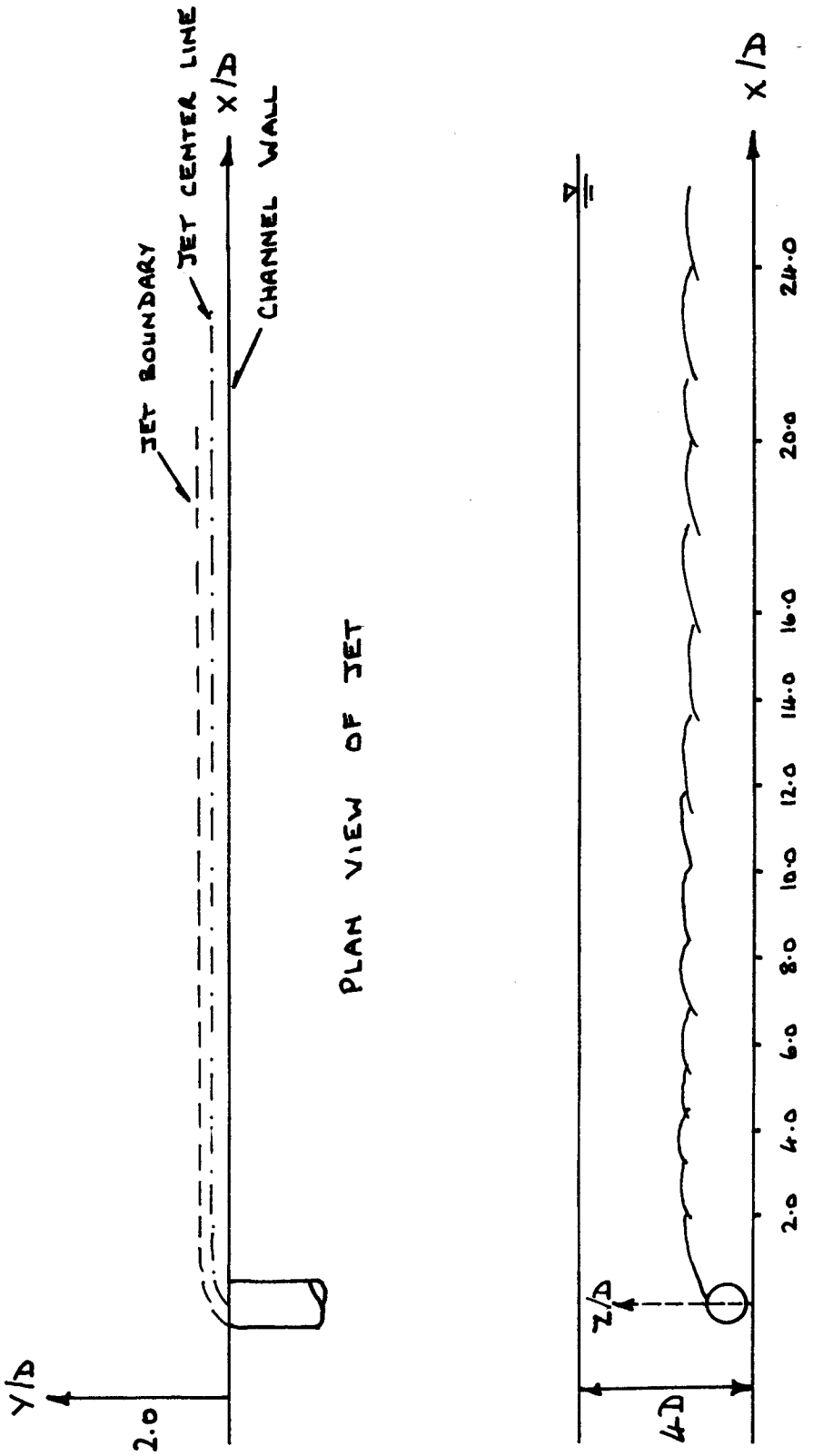

Figure 18. Jet Side Elevation and Plan View for B = 0.5, L/D = 0.0.

whether the discharge conduit protrudes into the free stream or not is not a factor in the jet trajectory unless B < 1.

Figure 19 has been included to provide limited comparison of the present data with some other published results for (class 3) non-buoyant jets into cross flows. The equation and corresponding dashed-line curve in Fig. 19 were proposed by Chan and Kennedy (1972) as a suitable empirical representation of the near-field trajectory of a non-buoyant jet entering a cross flow at a right angle; the equation was based upon their data and upon data obtained earlier by other investigators. The L/D = 10 configuration was selected for the comparison. The spread of the present data for the various B ratios can be interpreted only on the basis of effects of the finite channel in confining the flow plus, of course, the fundamental difference between the class 3 and class 4(c) jets. The present data follow the same trends, and straddle, the non-buoyant jet trajectories. Another comparison, made but not plotted in this report, gives comparable results in the 'curvilinear' zone out to x/BD and y/BD values of about 1.5. The general results are intuitively acceptable for most cases in that the trajectories of the jets in the present study follow general curvatures much like those of non-buoyant jets in cross-flows, but tend to have smaller y-displacements for equal x-displacements for comparable B values. The comparison for B = 0.5 is not a valid one because of the effect of the protruding conduit, as already discussed.

Centerline Temperature

Temperature data presented in this report are limited to jet centerline values. The experimental procedures were outlined in Section III. The incomplete specification of the temperature field was selected in interests of project economy, and also because of the increased lateral spreading of

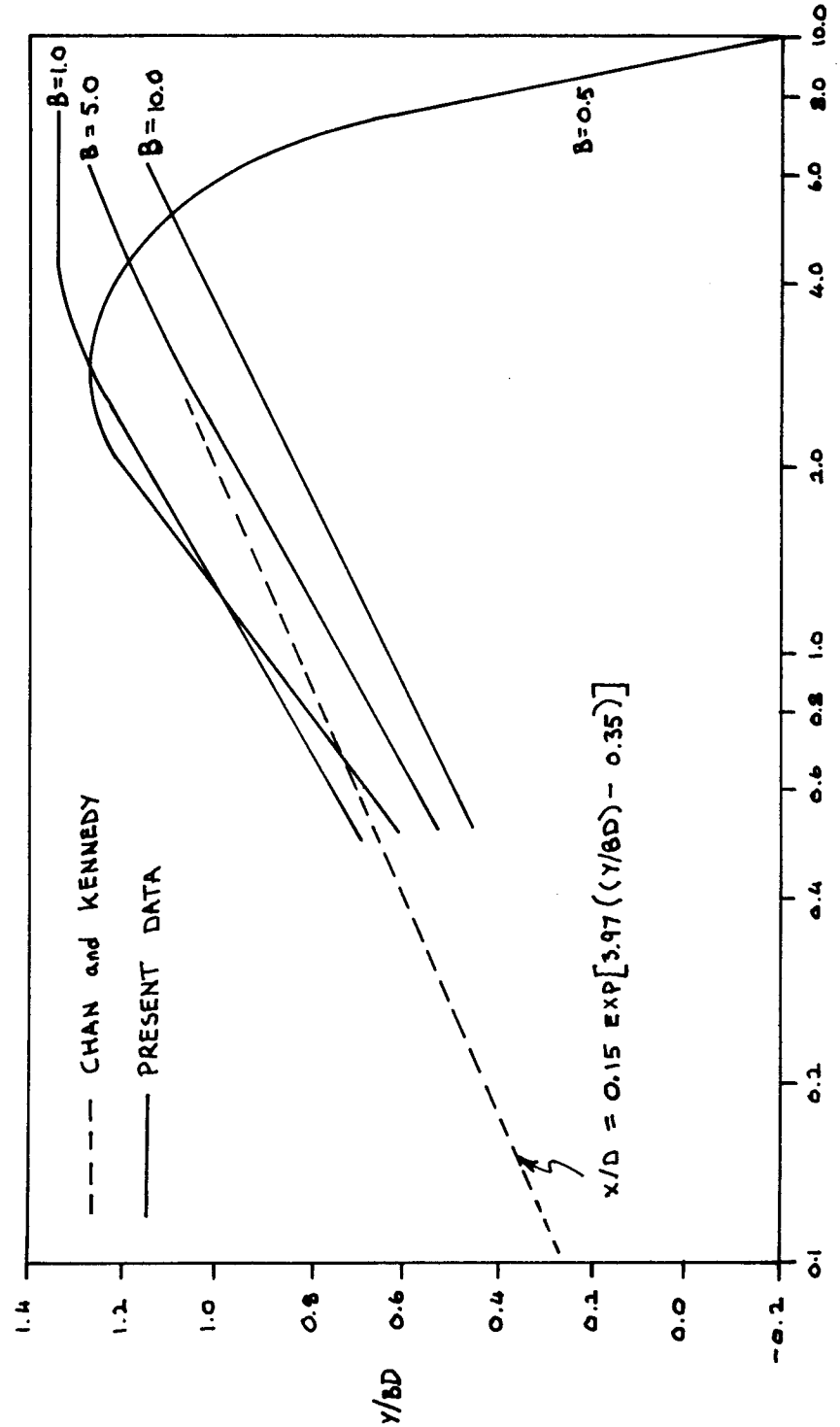

Figure 19. Logarithmic Jet Profiles in the Near Field Zone.

the jet and its associated temperature field caused by the jet being confined in the relatively shallow cross flow stream of d/D = 4. It did not seem reasonable to expand details of the temperature field because the results could not be generally applicable due to the confining boundary conditions which have been discussed in some detail. The lateral spread of temperature elevations would be greater than that in an infinitely deep receiving channel, all other parameters being kept equal; the photograph Fig. 5, for example, shows a greater lateral spread than is seen in photographs of other jets directed into cross flows of relatively much larger cross-sectional area. Although the temperature results in some cases are given for points on the jet trajectory downstream of surface 'boil' locations, no attempt was made to consider any effects of heat transfer to the air. Correlation of the dimensionless temperature parameter T with the axial distance s/D was selected not only to facilitate any possible comparisons with other data in the literature(centerline values might give a better correlation than would the temperature spread) but also because s represents more precisely the distance along which mixing and diffusion take place.

The variation of the temperature elevation parameter T with distance along the jet centerline is shown in Figs. 20, 21, 22, and 23 for velocity ratios B of 0.5, 1, 5, and 10, respectively, for the L/D = 10 configuration. Each figure shows the curves for the various nominal $\mathbb{F}$ values for each B value and also shows a dashed curve representing the average, or composite, result. Once again, as for the jet trajectories, the $\mathbb{F}$ value is seen to have no significant effect; the velocity ratio B governs.

The four 'average' curves are plotted in Fig. 24, along with the curve obtained for a single run at B = 2.5. The experimental results appear to follow the same general trends, although there is inconsistency in the data for

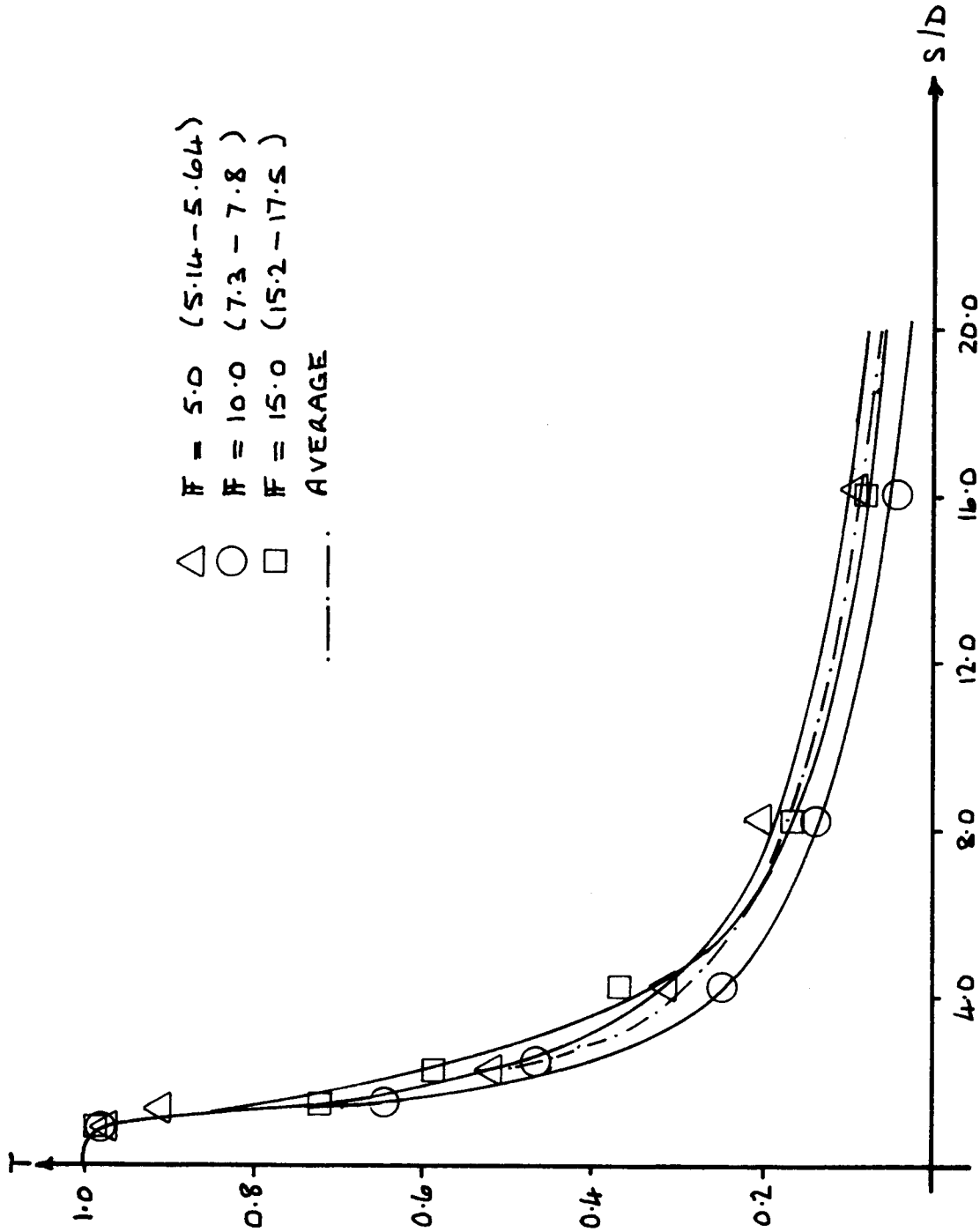

Figure 20. Plots of T Vs. Distance Along Jet Centerline Trajectories B = 0.5, L/D = 10.0 and Variable F.

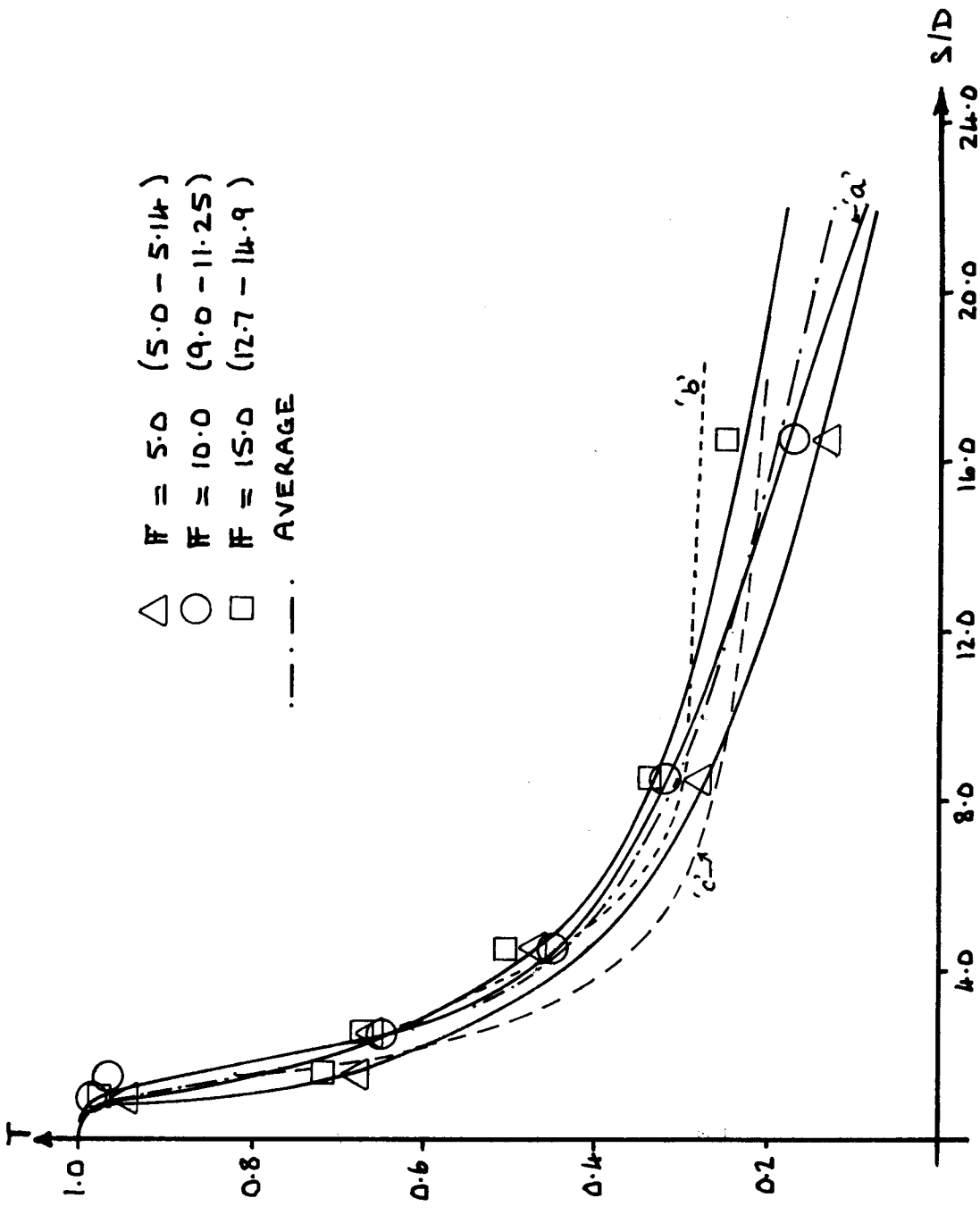

Figure 21. Plot of T Vs. Distance Along Jet Centerline Trajectories for B = 1.0, L/D = 10.0 and Variable FF.

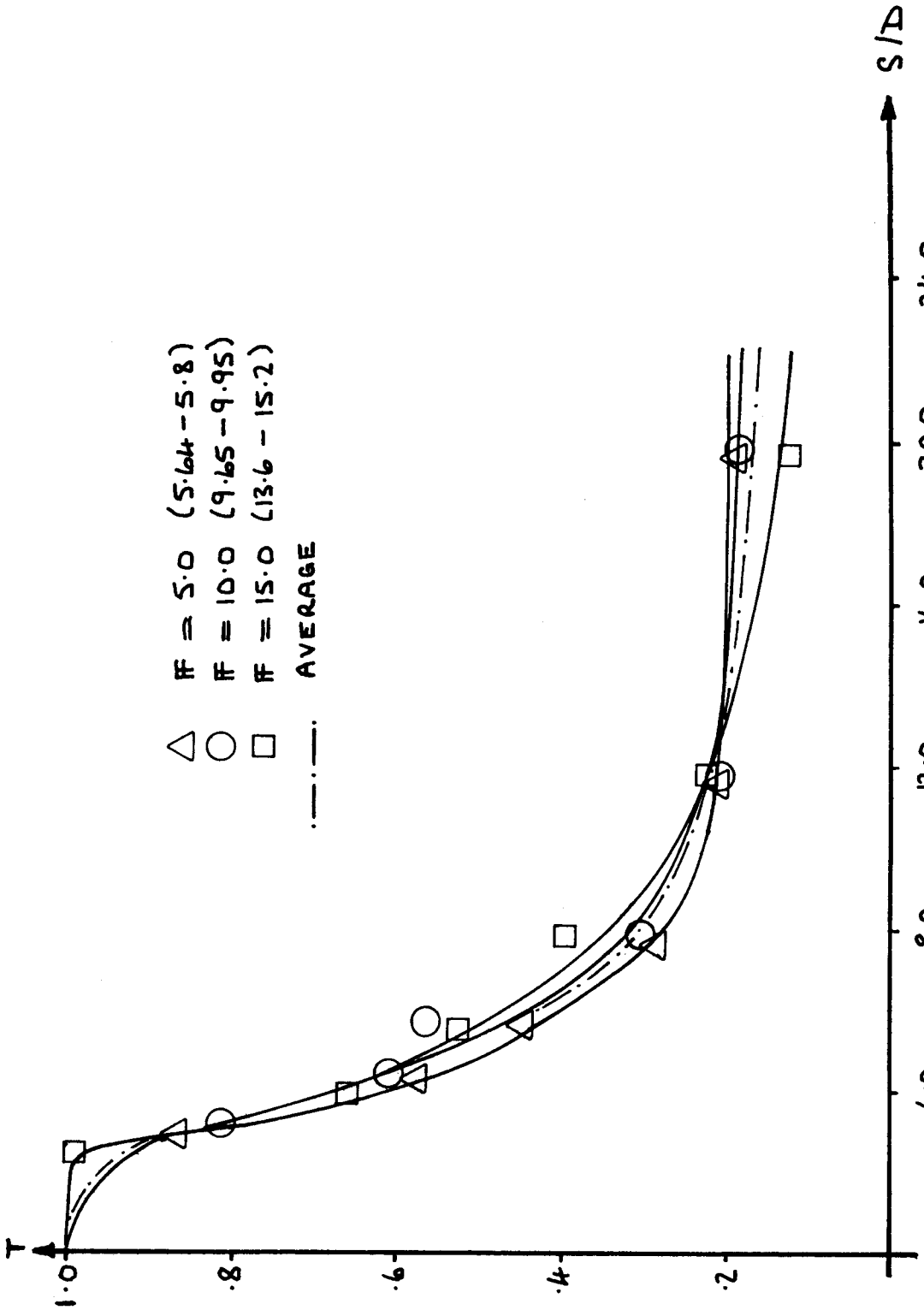

Figure 22. Plot of T Against Distance Along Jet Centerline Trajectories for B = 5.0, L/D = 10.0 and Variable FF.

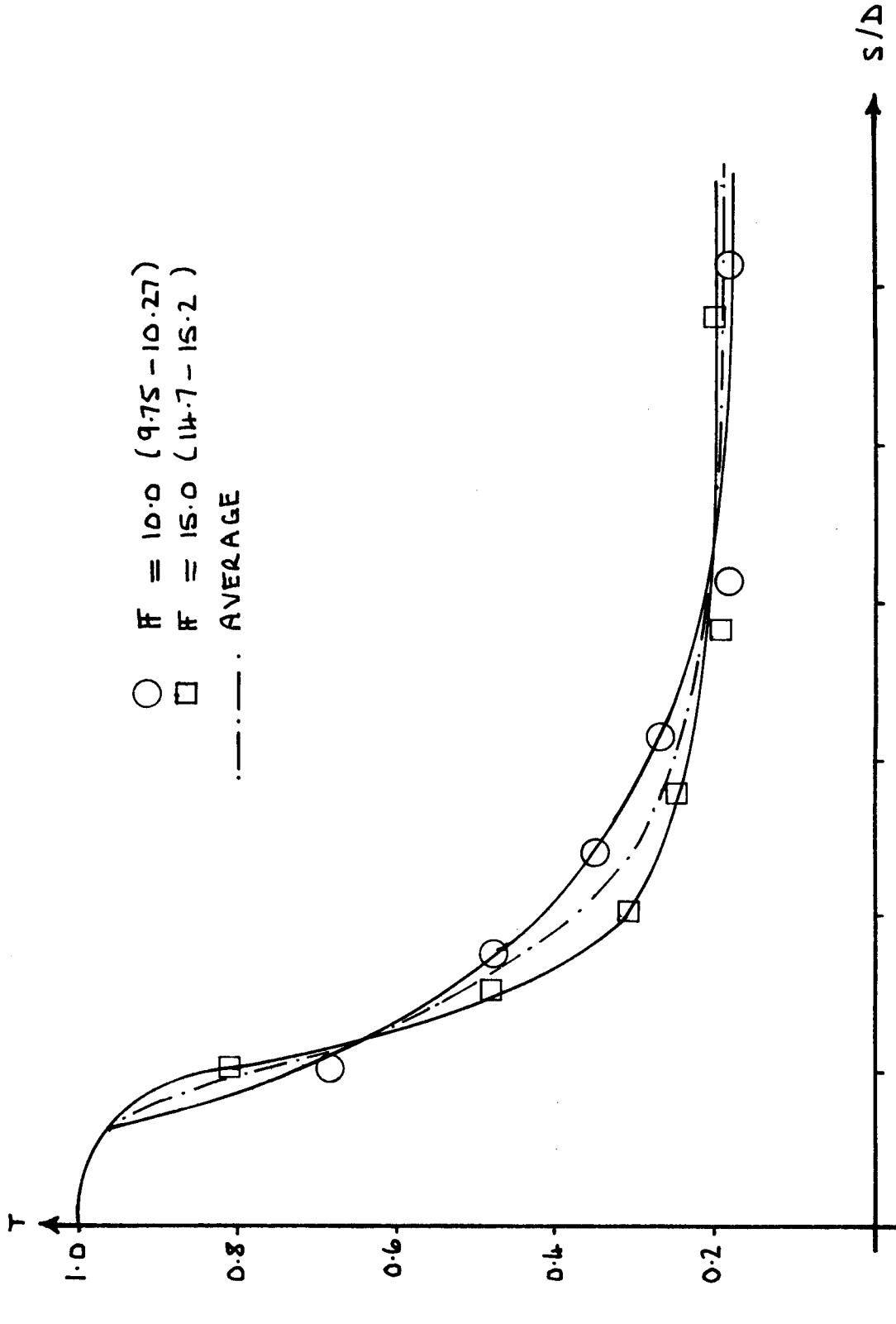

Figure 23. Plots of T Vs. Distance Along Jet Centerline Trajectories for B = 10.0, L/D = 10.0 and Variable FF.

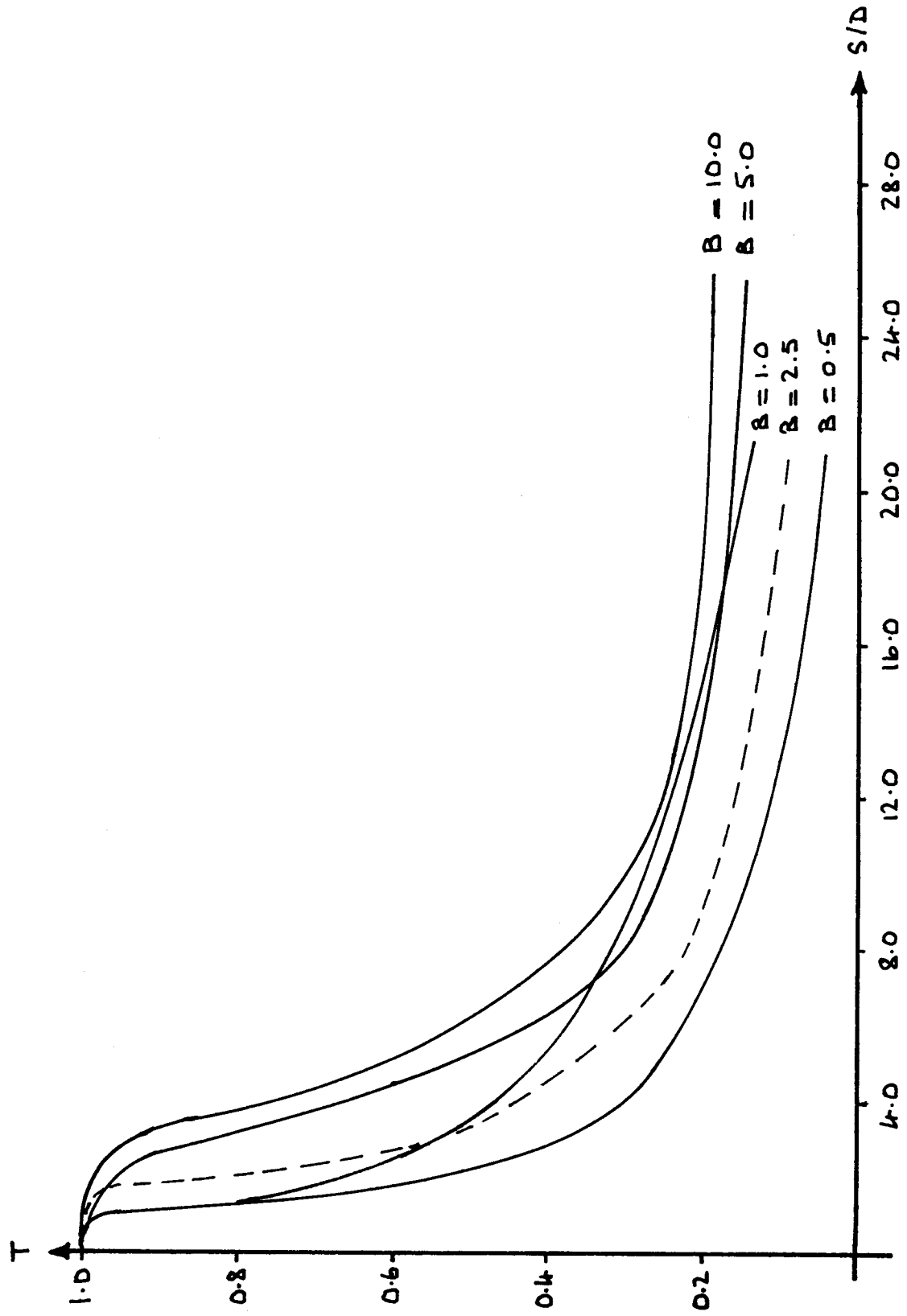

Figure 24. Plots of T Vs. Distance Along Jet Centerline Trajectories Representing Average Curves for Various Velocity Ratios, L/D = 10.

B = 1 and B = 2.5.

The data plotted on Fig. 21 for the $\mathbb{F}$ = 10 case are for original run 'a'; the curves for the procedural check runs 'b' and 'c' discussed in the preceding section are indicated by dashed lines. The results of the temperature data for these repeat runs at $\mathbb{F}$ = 10, B = 1 are isolated in Fig. 25. Considering the instrumental accuracy available, the agreement between the curves on Fig. 25 can be considered adequate. Although temperatures were measured and T values plotted in Figs. 20-23 for s/D values as large as 24, the actual data may not be as reliable at the most downstream measurement station, x/D = 16. As the accuracy and readability of the telethermometer were the values given in Section III, and as temperature differences $T_{\ell} - T_a$ of as low as 1.4°C were experienced at x/D = 16, possible errors in computed T values are significant.

The curves of Fig. 25 have been reproduced on the logarithmic plot of Fig. 26. Also given on this figure, for s/D > 5.6, the dashed curve which has the equation

$$T = \frac{T_{\ell} - T_a}{T_o - T_a} = 5.6 \left(\frac{s}{D}\right)^{-1} \tag{10}$$

which is the same as Eq. 6 but with temperature differentials substituted for concentrations, applied to a jet discharging into a quiescent receiving fluid. The equivalent velocity ratio is B = ∞. In general the present data follow the same extinction of centerline concentration with axial distance s, but with the potential core length becoming shorter with decreasing B. With increasing B, results approach closer to the limiting case given by Eq. 10. The unresolved behavior of the results for B = 1 and 2.5 is again emphasized.

Figures 27, 28, 29, and 30 show the centerline T values for the B values

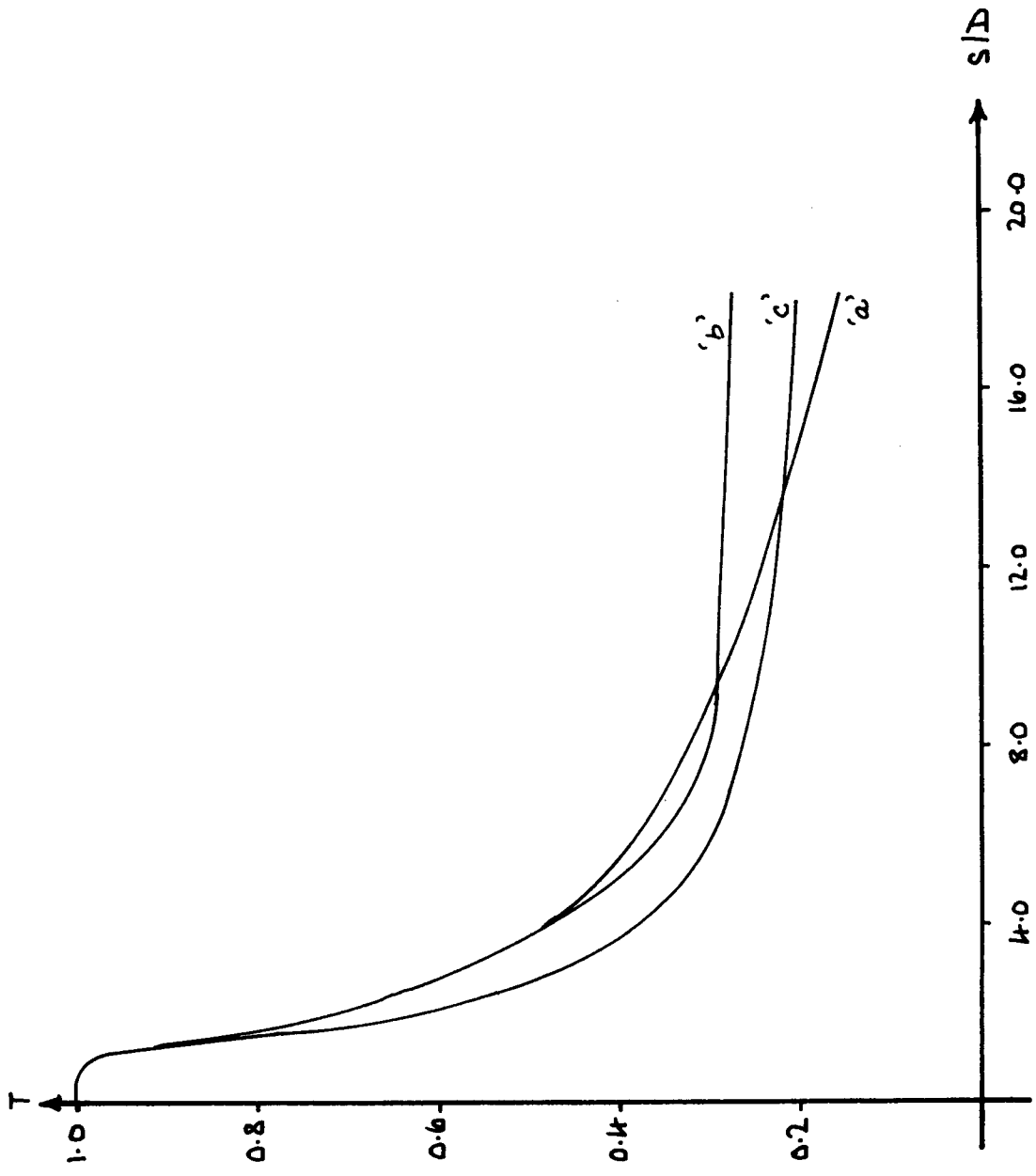

Figure 25. Plots of T Vs. Distance Along Jet Centerline Trajectory for Three Separate Runs Duplicating B = 1.0, $\overline{H}$ = 10.0, L/D = 10.0.

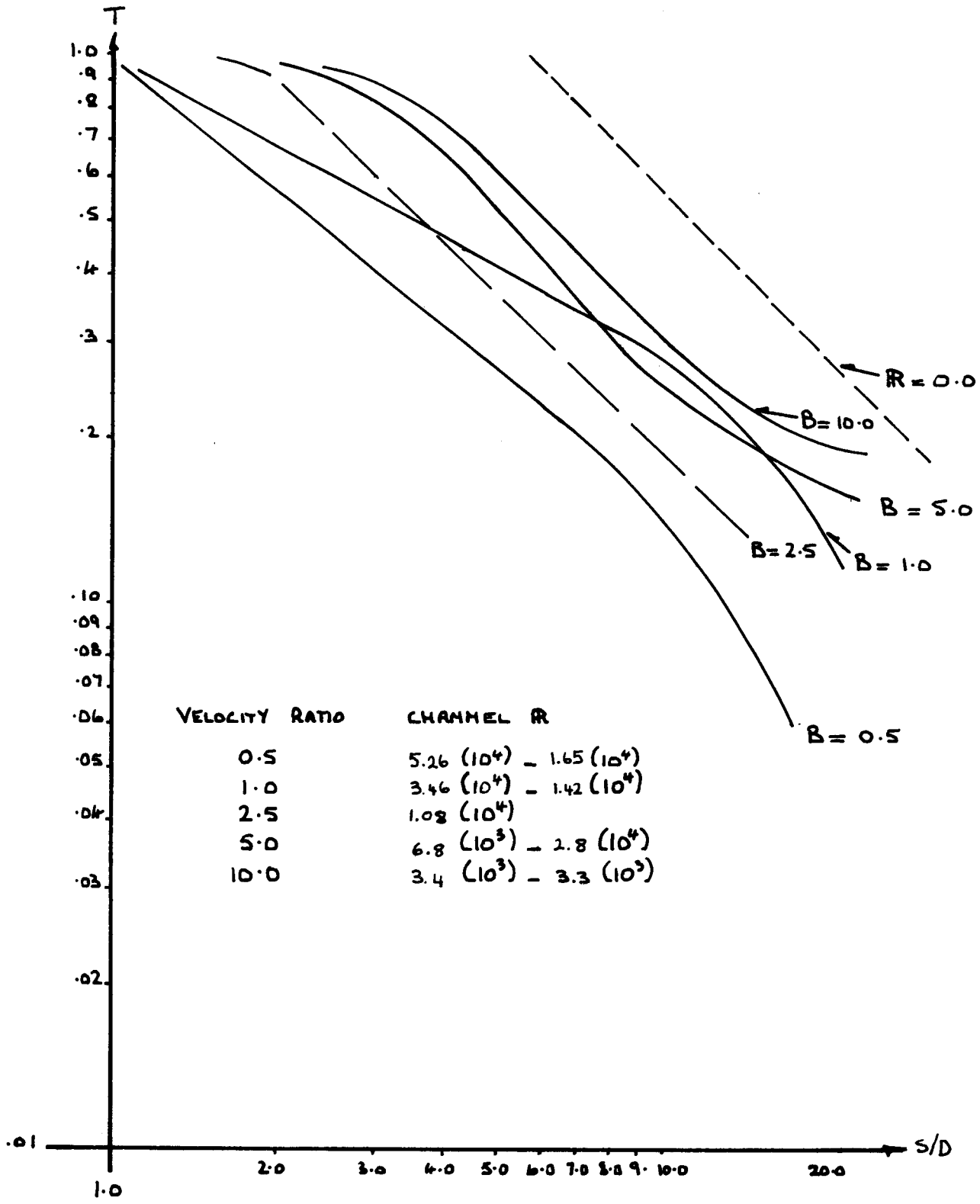

Figure 26. Logarithmic Plot of Average Curves of Temperature Parameter Variance with Distance Along Jet Centerline Trajectory for L/D = 10.0.

of 0.5, 1, 5, and 10 respectively for the L/D = 0 layout. These results are compared with the average centerline T curves for the corresponding velocity ratios B at L/D = 10. The same conclusions apply as for the jet trajectory data discussed before. Only for the low value of B = 0.5 did the presence of the nearby sidewall have any significant effect. The reduced mixing of the jet in the L/D = 0 case is evident from the higher jet centerline temperatures downstream. There was little effect of $\mathbb{F}$ on centerline temperature decay. The results in Figs. 28-30, taken at the nominal $\mathbb{F}$ = 10, indicate close agreement between results for L/D = 10 and L/D = 0.

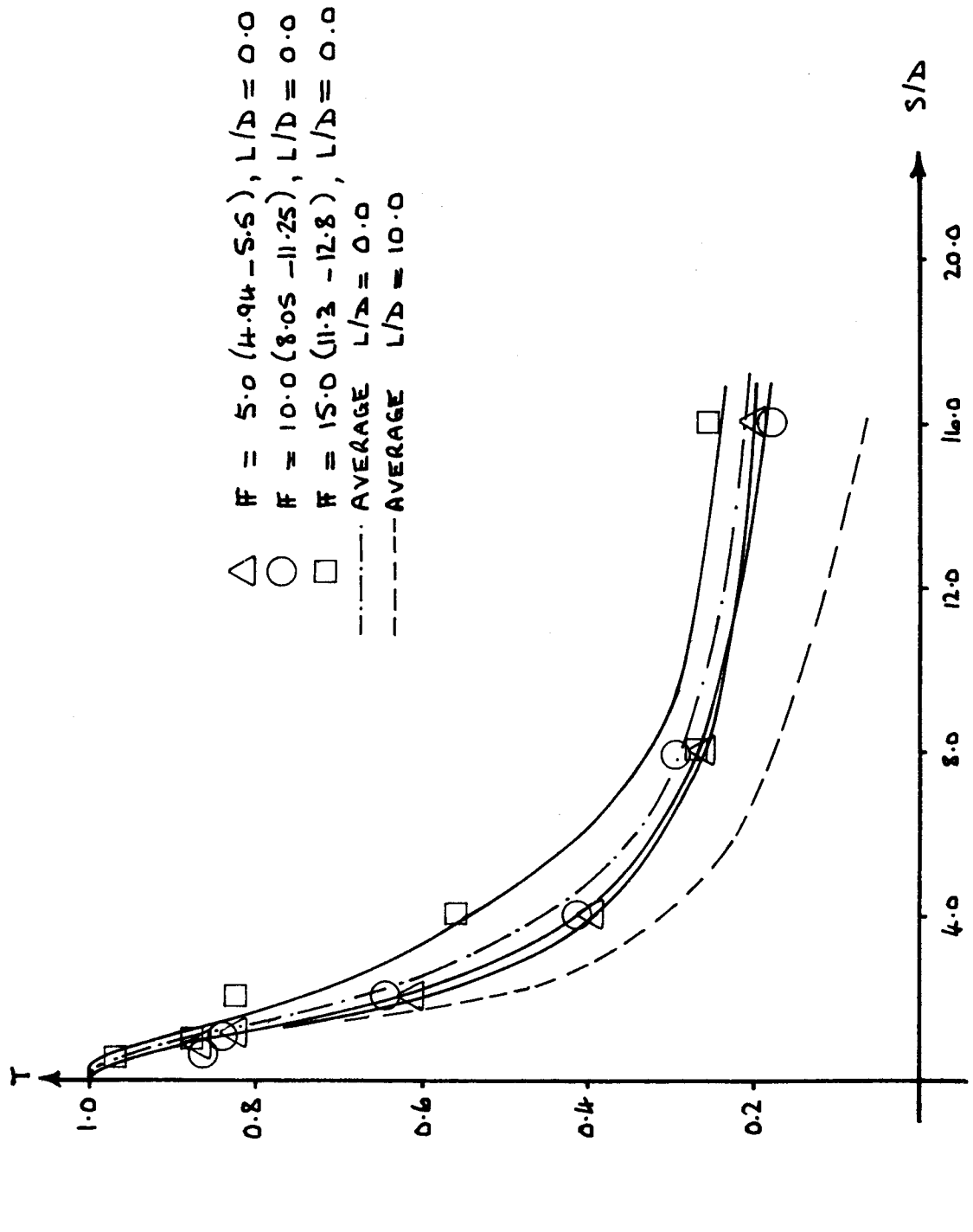

Figure 27. Comparison of Plots of T Variation Along Jet Centerline Trajectory for B = 0.5, L/D = 0.0 and B = 0.5, L/D = 10.0.

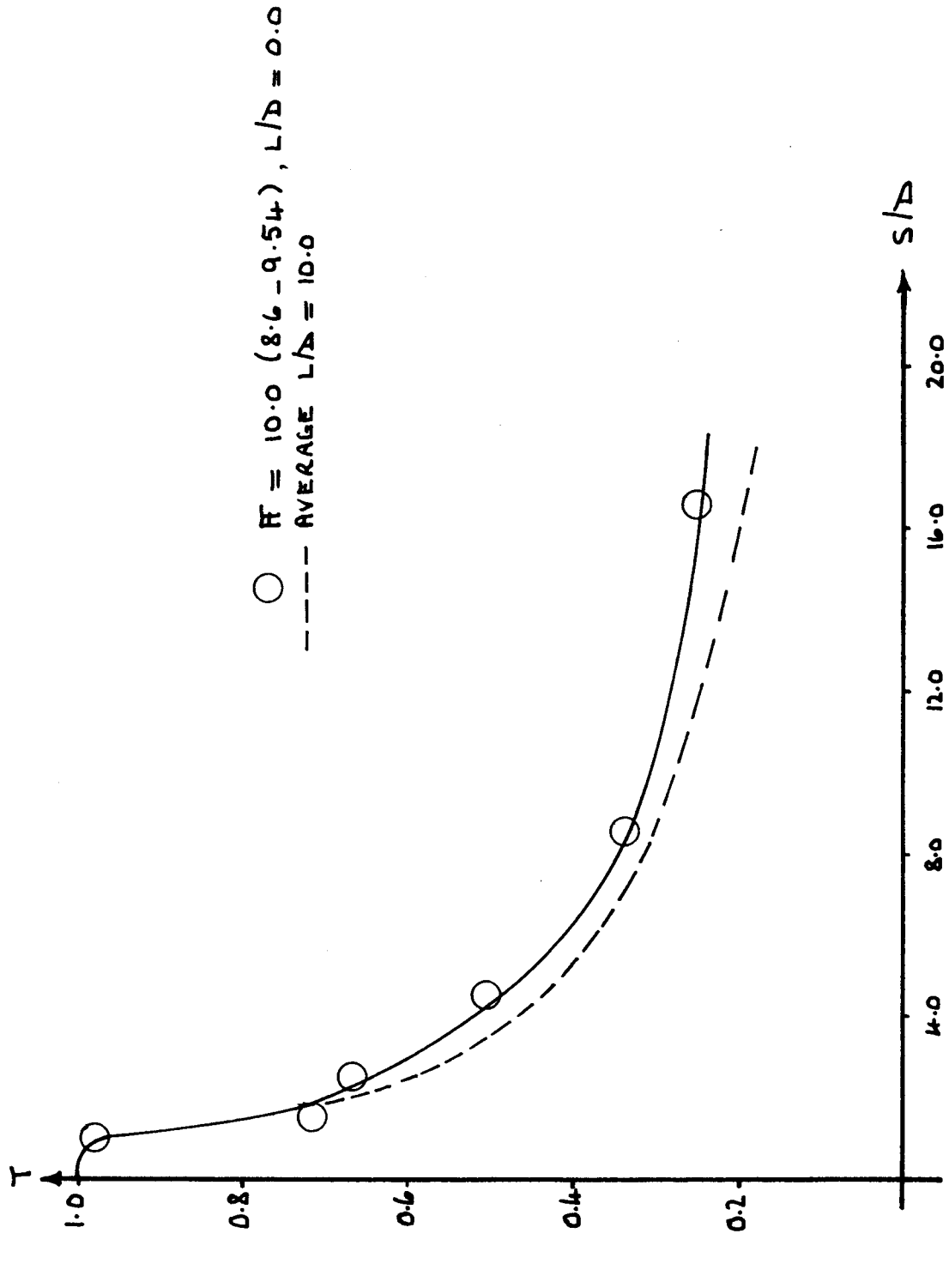

Figure 28. Comparison of Plots of T Variation Along Jet Centerline Trajectory for B = 1.0, L/D = 0.0 and B = 1.0, L/D = 10.0.

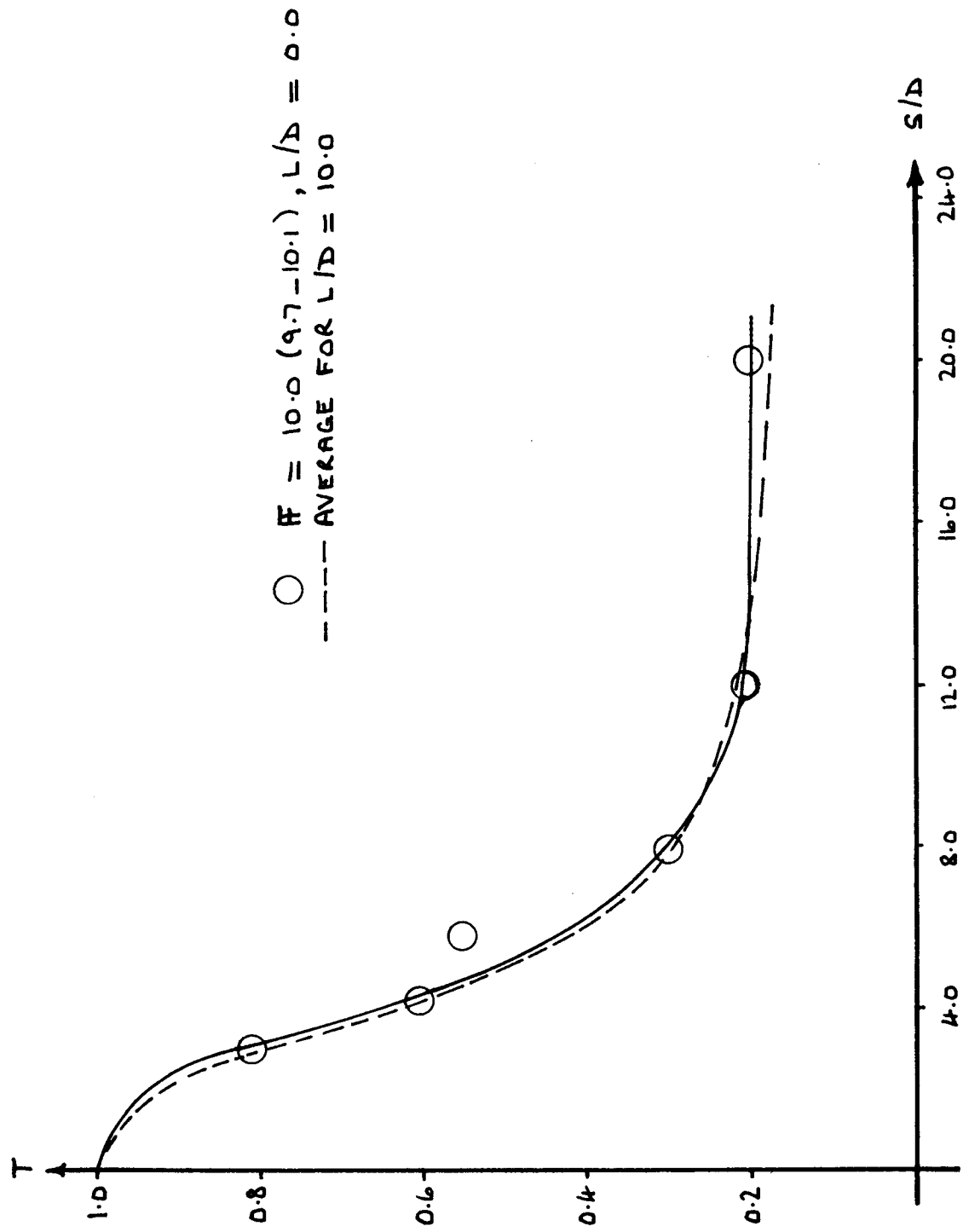

Figure 29. Comparison of T Variation Along Jet Centerline Trajectory for B = 5.0, L/D = 0.0 and B = 5.0, L/D = 10.0.

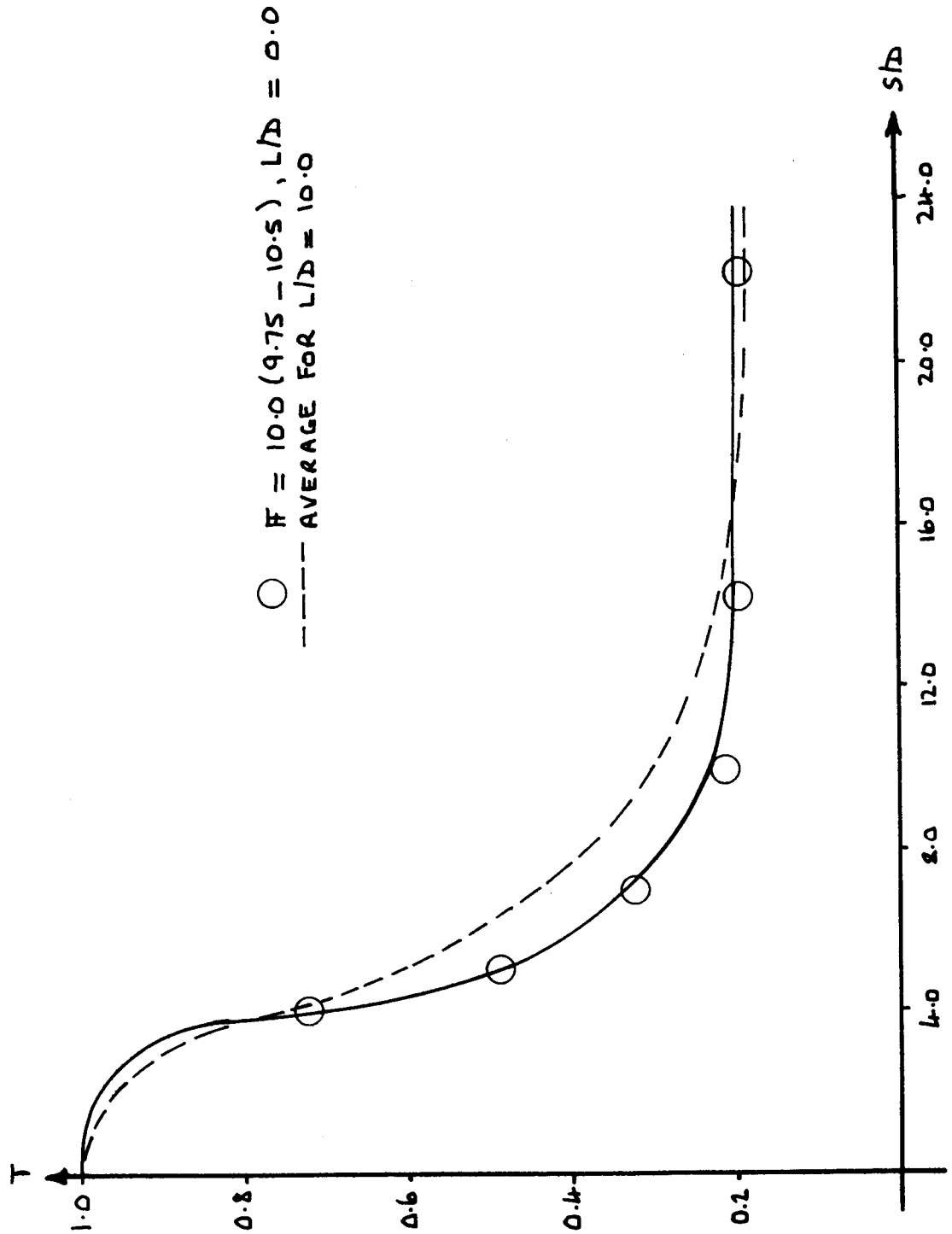

Figure 30. Comparison of T Variation Along Jet Centerline Trajectory for B = 10.0, L/D = 0.0 and B = 10.0, L/D = 10.0.

V. CONCLUSIONS

From the results of this study it is evident that the governing factor with respect to the behavior of a class 4(c) buoyant jet discharged at right angles into a cross flow is the velocity ratio B and not the densimetric Froude number F, which characterizes the behavior of buoyant jets discharged into a quiescent receiving fluid.

Downstream, in the vertically confined cross flow of the test program, jet centerline temperatures decayed more rapidly than would be the case of jets of $B = \infty$ discharging into receiving fluids at rest. The lateral temperature distribution (normal to the jet centerline) becomes more uniform and the jet experiences a comparably increased lateral spread rate in order to transport heat away from the nozzle and into the receiving cross flow.

The present data cannot be considered as fully general because of the nature of the boundaries confining the cross flow. However, as the jet trajectories behaved much like those of non-buoyant jets in cross flows, the limited data do suggest the following approach to be reasonable for predicting temperature distributions in the near field for round, horizontal thermal-buoyant jets discharged at right angles into an unstratified cross flow:

(1) Use the non-buoyant jet trajectory equations such as those given by Pratte and Baines (1967) or by Chan and Kennedy (1972) to predict the jet trajectory.

(2) Use the concentration distribution calculation procedures and data given by Fan (1967), transposed to temperatures, to estimate temperature distributions in the jet cross-section.

The work reported here can be classified as only a preliminary study. The following suggestions are made for necessary future work to generalize

more the behavior of the jets examined:

(1) Conduct similar tests, with minimized physical boundary effects. This could be done in the rig used here by using much smaller jet conduits and employing finer meshes on the temperature distribution plots. Perhaps the effects of d/D and z_o/D, both of which might be significant in an actual design situation, could be isolated. Channel and jet Reynolds numbers could be reduced, and likewise turbulence levels in the cross flow.

(2) More and careful data should be taken in the range $1 < B < 2.5$ in order to tie down whether or not significant changes in jet characteristics do occur, in this range of the jet velocity: cross flow velocity ratio.

VI. REFERENCES

Abraham, G. 1960. "Jet Diffusion in Liquid of Greater Density", Proc. ASCE, Journal of the Hydraulics Division, 86, No. HY6, June, 1-13.

Abramovich, G.N. 1963. "The Theory of Turbulent Jets", M.I.T. Press, Cambridge, Mass.

Albertson, M.D., Y.B. Dai, R.A. Jensen and H. Rouse, 1950. Transactions ASCE, 115, 639-664.

Anwar, H.O., 1969. "Behavior of Buoyant Jet in Calm Fluid", Proc. ASCE, Journal of the Hydraulics Division, 95, No. HY4, July, 1289-1303.

Chan, T.-L. and J.F. Kennedy, 1972. "Turbulent Nonbuoyant or Buoyant Jets Discharged into Flowing or Quiescent Fluids", Iowa Institute of Hydraulic Research Report No. 140, University of Iowa, Iowa City, Iowa, August, 153 pp.

Fan, L.-N. 1967. "Turbulent Buoyant Jets into Stratified or Flowing Ambient Fluids", W.M. Keck Laboratory of Hydraulics and Water Resources Report No. KH-R-15, California Institute of Technology, Pasadena, California, June, 196 pp.

Fan, L.-N. and N.H. Brooks, 1966. Discussion of "Horizontal Jets in Stagnant Fluid of Other Density", Proc. ASCE, Journal of the Hydraulics Division, 92, No. HY2, March, 423-429.

Fan, L.-N. and N.H. Brooks, 1969. "Numerical Solutions of Turbulent Buoyant Jet Problems", W.M. Keck Laboratory of Hydraulics and Water Resources Report No. KH-R-18, California Institute of Technology, Pasadena, California, January, 94 pp.

Hirst, E., 1972. "Buoyant Jets with Three-Dimensional Trajectories", Proc. ASCE, Journal of the Hydraulics Division, 98, No. HY11, November, 1999-2014.

Lomax, C.C., 1971. "Dispersion of Thermal Effluents", College of Engineering Research Division Bulletin No. 323, Washington State University, Pullman, Wash., 65 pp.

Nece, R.E. and J.C. Kent, 1971. "Hydraulic Modeling Study: Simulated Juvenile Salmon Migration Past Cooling-Water Discharge Jet", Charles W. Harris Hydraulics Laboratory Tech. Report No. 31, July, 34 pp.

Pratte, B.D. and W.D. Baines, 1967. "Profiles of the Round Turbulent Jet in a Cross Flow", Proc. ASCE, Journal of the Hydraulics Division, No. HY6, November, 53-64.

Rouse, H., C.S. Yih and H.W. Humphreys, 1952. "Gravitational Convection from a Boundary Source", Tellus, 4, No. 3, August, 201-210.

L/D	10	10	10	10	10	10	10
U_0 - fps	.5	.8	.75	.50	.81	.81	.5
V - fps	1.0	1.6	1.5	.50	.80	.80	.5
R-Channel (10^4)	2.82	5.26	4.25	1.65	2.64	2.26	1.42
R-Jet (10^4)	.59	1.14	.72	.63	1.01	.96	.51
F	5.0	10.0	15.0	5.0	10.0	10.0	10.0
B	.5	.5	.5	1.0	1.0	1.0	1.0
T_a (°C)	10.5	14.9	10.6	16.0	15.2	9.0	10.5
T_0(°C) at x/D = 0.5	22.0	28.5	15.0	27.0	28.3	21.0	15.2
1.0	22.0	28.2	14.75	26.4	27.5	21.0	14.8
2.0	22.5	28.8	14.5	26.4	26.5	23.0	14.5
4.0	23.3	29.2	16.0	26.8	26.5	22.1	15.0
8.0	23.0	29.6	16.0	27.0	26.8	21.8	13.3
16.0	24.0	29.6	15.5	27.0	26.5	21.5	11.6
Tc_L(°C)at x/D = 0.5	21.9	28.9	14.9	26.4	28.2	20.7	15.0
1.0	21.0	24.5	13.4	23.0	24.0	18.0	13.9
2.0	16.4	23.0	12.4	22.8	23.0	18.2	13.0
4.0	14.5	20.0	12.0	21.0	20.0	14.7	12.0
8.0	13.0	17.2	11.5	19.0	18.7	12.2	11.9
16.0	11.7	16.0	11.0	17.4	17.0	10.3	11.6
T at x/D = 0.5	.99	.99	.98	.95	.99	.98	.96
1.0	.91	.72	.65	.67	.71	.75	.77
2.0	.51	.58	.46	.65	.69	.66	.63
4.0	.31	.37	.25	.46	.43	.44	.33
8.0	.20	.16	.14	.27	.30	.30	.27
16.0	.09	.08	.04	.13	.16	.28	.20
$(y/D)c_L$ at x/D = 0.5	.48	.24	.40	1.00	1.0	.48	.56
1.0	.56	.40	.44	1.04	1.28	.72	.88
2.0	.64	.80	.52	1.44	1.44	.88	1.04
4.0	.68	.80	.48	1.52	1.60	1.20	1.36
8.0	.20	.18	.16	1.68	1.60	1.20	1.28
16.0	-.64	-.40	-1.6	1.68	1.60	1.10	1.20
$(S/D)c_L$ at x/D= 0.5	.75	.625	.75	1.5	1.0	1.0	1.0
1.0	1.30	1.70	1.20	2.0	1.5	1.6	1.6
2.0	2.25	2.47	2.30	3.0	2.5	2.6	3.0
4.0	4.25	4.47	4.25	5.0	4.5	4.6	5.0
8.0	8.30	7.47	8.20	9.0	9.5	9.6	9.0
16.0	16.20	15.47	16.20	17.0	16.5	16.6	17.0
					'a'	'b'	'c'

L/D		10	10	10	10	10	10	10
U_0 - fps		1.22	.81	.50	.81	1.22	1.0	1.2
V - fps		1.22	.33	.10	.16	.24	.1	.12
ℜ-Channel (10^4)		3.46	1.08	.28	.45	.68	.33	.34
ℜ-Jet (10^4)		1.53	1.02	.59	1.02	1.45	1.26	1.42
ℱ		15.0	10.0	5.0	10.0	15.0	10.0	15.0
B		1.0	2.5	5.0	5.0	5.0	10.0	10.0
T_a (°C)		9.0	15.0	9.5	11.6	8.5	15.0	10.0
T_0(°C) at x/D =	0.5	23.3	28.3	21.5	23.0	21.5	27.0	20.1
	1.0	23.2	27.5	22.5	23.0	21.9	26.2	19.9
	2.0	23.0	26.8	22.0	23.0	22.1	25.8	19.8
	4.0	23.0	26.0	21.8	23.0	20.3	25.2	20.0
	8.0	21.2	25.3	21.7	23.0	20.2	26.0	20.2
	16.0	21.0		21.0	22.0	20.1	26.0	19.8
Tc_L(°C) at x/D=	0.5	23.0	28.0	20.0	21.0	21.5	23.2	18.2
	1.0	20.1	24.0	17.0	17.0	17.2	20.4	14.8
	2.0	18.0	21.0	15.1	17.0	15.2	18.8	13.0
	4.0	15.2	19.0	13.0	13.5	13.2	17.8	12.5
	8.0	12.9	17.0	12.0	13.0	11.0	17.0	12.0
	16.0	11.0		11.9	12.0	10.0	17.0	12.0
T at x/D	= 0.5	.98	.98	.88	.80	.99	.68	.81
	1.0	.97	.72	.58	.48	.66	.48	.49
	2.0	.65	.51	.45	.46	.53	.35	.31
	4.0	.44	.36	.29	.20	.40	.27	.25
	8.0	.32	.20	.21	.19	.22	.18	.20
	16.0	.17		.20	.15	.13	.18	.20
$(y/D)c_L$ at x/D=	0.5	.56	1.68	2.72	3.00	2.32	4.40	4.72
	1.0	1.08	1.92	4.08	3.92	3.60	6.73	6.07
	2.0	1.04	2.60	5.28	4.96	4.40	8.70	7.92
	4.0	1.04	3.00	5.84	6.40	5.44	11.10	10.2
	8.0	1.20	3.60	6.40	7.0	6.42	12.0	12.0
	16.0	1.12		7.20	7.3	6.40	12.8	13.6
$(s/D)c_L$ at x/D=	0.5	1.0	1.75	2.5	3.0	2.5	4.25	4.0
	1.0	1.6	2.25	4.0	4.0	3.75	6.50	6.0
	2.0	3.0	3.25	5.5	5.5	5.0	8.75	8.25
	4.0	5.0	5.25	7.5	8.0	7.25	11.75	11.25
	8.0	9.0	9.25	11.5	12.0	11.25	15.75	15.50
	16.0	17.0		19.5	20.0	19.25	23.75	23.50

L/D		0	0	0	0	0	0
U_o - fps		.5	.6	.75	.8	.81	1.0
V - fps		1.0	1.2	1.5	.8	.16	.1
ℜ-Channel (10^4)		2.80	3.40	4.26	2.3	.45	.33
ℜ-Jet (10^4)		.63	.71	.88	.94	.96	1.26
℉		5.0	10.0	15.0	10.0	10.0	10.0
B		.5	.5	.5	1.0	5.0	10.0
T_a (°C)		11.4	10.8	10.1	11.2	11.9	16.0
T_0(°C) at x/D =	0.5	25.0	18.0	18.5	23.0	22.0	25.0
	1.0	24.2	17.0	18.0	23.0	21.8	26.0
	2.0	24.0	17.0	17.0	22.9	21.8	26.8
	4.0	23.5	16.5	17.0	22.8	22.0	29.0
	8.0	23.5	16.9	17.3	22.2	22.0	27.9
	16.0	23.9	17.2	16.8	22.2	21.6	25.0
Tc_L(°C) at x/D =	0.5	23.0	17.0	18.2	22.7	20.1	22.5
	1.0	21.8	16.0	17.0	19.6	17.9	20.9
	2.0	19.0	14.8	15.8	19.0	16.5	18.2
	4.0	16.1	13.2	13.9	17.0	15.0	17.2
	8.0	14.5	12.5	12.2	14.9	14.0	16.0
	16.0	13.9	12.0	11.8	13.9	13.9	15.4
T at x/D =	0.5	.85	.86	.97	.98	.81	.72
	1.0	.81	.84	.87	.71	.61	.49
	2.0	.60	.64	.83	.67	.57	.33
	4.0	.39	.41	.55	.50	.31	.21
	8.0	.26	.27	.29	.34	.21	.20
	16.0	.20	.18	.25	.25	.21	.20
$(y/D)c_L$ at x/D =	0.5	.32	.28	.32	.76	3.16	4.00
	1.0	.36	.36	.32	.80	4.24	5.12
	2.0	.40	.36	.36	1.1	5.60	6.80
	4.0	.40	.36	.36	1.3	6.55	9.05
	8.0	.40	.32	.40	1.3	6.64	10.70
	16.0	.40	.32	.36	1.7	7.44	12.0
$(s/D)c_L$ at x/D =	0.5	.75	.75	.75	1.0	3.25	4.0
	1.0	1.25	1.25	1.25	1.50	4.50	5.25
	2.0	2.25	2.25	2.25	2.50	6.25	7.25
	4.0	4.25	4.25	4.25	4.50	8.50	10.25
	8.0	8.25	8.25	8.25	8.50	12.50	14.25
	16.0	16.25	16.25	16.25	16.50	20.50	22.25